Arabidopsis mTERF9 protein promotes chloroplast ribosomal assembly and translation by establishing ribonucleoprotein interactions *in vivo*.

Louis-Valentin Méteignier[1], Rabea Ghandour[2], Aude Zimmerman[1], Lauriane Kuhn[3], Jörg Meurer[4], Reimo Zoschke[2], Kamel Hammani[1]

[1]Institut de Biologie Moléculaire des Plantes, Centre National de la Recherche Scientifique (CNRS), Université de Strasbourg, 12 rue du Général Zimmer, 67084 Strasbourg, France

[2]Max Planck Institute of Molecular Plant Physiology, Am Mühlenberg 1, 14476 Potsdam-Golm, Germany

[3]Plateforme protéomique Strasbourg Esplanade FRC1589 du CNRS, Université de Strasbourg, 15 rue René Descartes, 67084 Strasbourg, France

[4]Plant Sciences, Faculty of Biology, Ludwig-Maximilians-University Munich, Großhaderner Street 2-4, 82152 Planegg-Martinsried, Germany

Corresponding author: Kamel Hammani, Email: kamel.hammani@ibmp-cnrs.unistra.fr

Short title: Plant mTERF involved in ribosome assembly

The author responsible for distribution of materials integral to the findings presented in this article in accordance with the policy described in the Instructions for Authors (www.plantcell.org) is: Kamel Hammani (kamel.hammani@ibmp-cnrs.unistra.fr)

ABSTRACT

The mitochondrial transcription termination factor proteins are nuclear-encoded nucleic acid binders defined by degenerate tandem helical-repeats of ~30 amino acids. They are found in metazoans and plants where they localize in organelles. In higher plants, the mTERF family comprises ~30 members and several of these have been linked to plant development and response to abiotic stress. However, knowledge of the molecular basis underlying these physiological effects is scare. We show that the Arabidopsis mTERF9 protein, promotes the accumulation of the 16S rRNA and the formation of the 23S rRNA first hidden break in chloroplasts, and co-immunoprecipitates with the 16S rRNA.

Furthermore, mTERF9 is found in large complexes containing ribosomes and polysomes in chloroplasts. The analysis of the *in vivo* mTERF9 protein interactome identified many ribosomal proteins whose assembly into 70S ribosomes is compromised in the null *mterf9* mutant. mTERF9 additionally interacts with putative ribosome biogenesis factors and CPN60 chaperonins. Yeast protein interaction assays revealed that mTERF9 has the capacity to directly interact with these proteins. Our data demonstrate that mTERF9 integrates protein-protein and protein-RNA interactions to promote chloroplast ribosomal assembly and translation. Besides extending our knowledge of mTERF molecular functions in plants, these findings provide important insight into the chloroplast ribosome biogenesis.

INTRODUCTION

The mitochondrial transcription termination factor (mTERF) proteins are tandem degenerate α-helical repeats proteins that are encoded by nuclear genomes of all eukaryotes except fungi (Linder et al., 2005). Each mTERF repeat spans ~30 amino acids that fold into two consecutive antiparallel α-helices followed by a shorter α-helix perpendicular to the first one (Jimenez-Menendez et al., 2010; Spahr et al., 2010; Yakubovskaya et al., 2010). The mTERF repeats stack together to form an elongated solenoid structure with a central groove capable of binding nucleic acids (Yakubovskaya et al., 2010). mTERF proteins typically harbor an N-terminal organellar transit peptide and localize to mitochondria or chloroplasts and are considered to be putative organellar gene regulators. Whereas metazoans have 3 to 4 mTERF members, some plant genomes encode more than 30 mTERF proteins (Linder et al., 2005; Kleine, 2012; Zhao et al., 2014). The functions of mTERF proteins were first characterized in metazoans showing that they influence mitochondrial gene transcription, DNA replication and ribosome biogenesis (reviewed in Kleine and Leister, 2015). In plants, several of these genes are essential for embryo viability (Tzafrir et al., 2004; Babiychuk et al., 2011; Bryant et al., 2011). Others have been linked to a variety of abiotic stress-responses (Zhao et al., 2014; Zhou et al., 2016; Xu et al., 2017; Robles et al., 2018; Nunez-Delegido et al., 2019) but how these genes trigger these responses in plants is not understood. Plant mTERFs are predicted to act in mitochondria or chloroplasts but knowledge about their roles in

organelles is scare. In fact, only five of the ~30 mTERF proteins found in angiosperms have been connected to their gene targets and functions in organelles. In Arabidopsis, mTERF5 (known as well as MDA1), mTERF6 and mTERF8 are chloroplast DNA binding proteins involved in the regulation of chloroplast gene transcription (Zhang et al., 2018; Ding et al., 2019; Xiong et al., 2020). mTERF5 stimulates the transcription initiation of *psbE* and *ndhA* genes (Ding et al., 2019; Méteignier et al., 2020) whereas mTERF8 and mTERF6 promote the transcription termination of *psbJ* and *rpoA*, respectively (Zhang et al., 2018; Xiong et al., 2020). mTERF6 has additionally been reported to affect the maturation of *trnI.2* but the reason for this effect remained unclear (Romani et al., 2015). Finally, mTERF15 and mTERF4 assist in RNA splicing of the *nad2-3* intron in Arabidopsis mitochondria and group II introns in maize chloroplasts, respectively. Therefore, the functional repertoire of mTERFs in plant organelles concerns the regulation of gene transcription and intron splicing. In Arabidopsis, the *mTERF9* gene (known as well as *TWIRT1*) encodes a chloroplastic mTERF protein that has been involved in the development of the shoot apical meristem (Mokry et al., 2011) and the plant acclimation to high salinity (Robles et al., 2015; Nunez-Delegido et al., 2019). However, the function of mTERF9 in chloroplasts was not further investigated and the molecular basis underlying its physiological effects on plants is unknown. Understanding the connection between *mTERF* genes and the plant response to abiotic stress would require the elucidation of their molecular functions in organelles. To this end, we examined the molecular defects in the *mterf9* mutant and characterized the primary functions of mTERF9 in Arabidopsis. We show that mTERF9 is required for chloroplast ribosomal assembly and therefore, translation. Our findings further reveal that mTERF9 promotes ribosomal assembly via ribonucleoprotein interactions *in vivo*. Finally, we demonstrate that mTERF9 interacts physically with the CPN60 chaperonin complex *in vivo* suggesting a functional cooperation between these proteins in chloroplast ribosome biogenesis and translation. This study provides molecular evidence for a connection between defective chloroplast protein synthesis and the plant salinity response.

RESULTS

mTERF9 is a chloroplast nucleoid-associated protein required for plant growth

To characterize the molecular function of mTERF9, we analyzed the Arabidopsis mutant *mterf9* that was previously reported to affect plant development (Robles et al., 2015). This mutant carries a T-DNA insertion in the fourth intron of the *mTERF9*/At5g55580 gene (Figure 1A). *mTERF9* encodes a 496 amino acid protein harboring seven tandem mTERF motifs that are preceded by a predicted N-terminal chloroplast transit peptide (Figure 1A). We confirmed the *mterf9* mutant phenotype at different developmental stages. *mterf9* plants exhibited a pale leaf pigmentation and a retarded growth phenotype compare to wild-type (WT), but remained fertile (Figure 1B). The introduction of a WT copy of the *mTERF9* gene under the control of the CaMV 35S promoter into *mterf9* fully restored the WT phenotype demonstrating that the mutant phenotype resulted from *mTERF9* disruption. RT-PCR analysis confirmed the lack of *mTERF9* full-length mRNA in *mterf9* and its restoration in the complemented *mterf9* plants (CP) (Figure 1C). The chlorotic phenotype displayed by *mterf9* suggests a potential loss of photosynthetic activity in the mutant. Therefore, the functional status of photosynthesis of the mutant was monitored using a pulse amplitude modulated system (Table 1). In all respects, the complemented lines showed characteristics comparable to the WT. The *mterf9* mutant displayed a decrease in photosystem II (PSII) activity as revealed by a reduced maximum quantum yield of PSII (0,70 vs 0,81; *mterf9* vs WT) and an increased minimum fluorescence value (Fo) (Table 1). Effective quantum yield of PSII measured in the steady state 5 min after induction was decreased from 0,73 in the WT to 0,58 in *mterf9* whereas non-photochemical quenching was not affected. Overall, photosystem I (PSI) activity was reduced by one third in mutant plants as compared to the WT and no PSI donor side limitation could be detected. Instead, the quantum yield of non-photochemical energy dissipation due to PSI acceptor side limitation was reduced by about a half. The data indicate and confirmed a pleiotropic photosynthetic deficiency in the *mterf9* mutant rather than a specific defect. To confirm the predicted chloroplast intracellular localization of mTERF9, we transiently expressed an mTERF9 protein fused to a C-terminal GFP in *Nicotiana benthamiana* leaves and examined leaf protoplasts by confocal microscopy. The results revealed that the fusion protein localizes to punctuated foci overlapping with the chloroplast chlorophyll autofluorescence and additionally, with the fluorescence of a co-expressed nucleoid-associated chloroplast protein, RAP fused with RFP (Kleinknecht

et al., 2014). These results indicate that mTERF9 functions in chloroplasts of plant cells where it associates with the nucleoid.

mTERF9 deficiency impairs chloroplast protein accumulation and translation

The pale leaf and defective photosynthesis phenotypes displayed by the *mterf9* mutant suggests an mTERF9 function related to chloroplast biogenesis. To investigate mTERF9 function in chloroplasts, we first analyzed the accumulation of representative subunits of chloroplast protein complexes by immunoblotting in the mutant. With the exception of the LHCB2 subunit from the nuclear-encoded light harvesting complex II, the results showed a ~50-75% decrease in the amount of chloroplast proteins tested (Figure 2A) in the *mterf9* compared to the WT and complemented plants (Figure 2A). We additionally confirmed the expression of the mTERF9 protein fused to a C-terminal 4xMyc tag in the complemented plants and showed its dual-detection in both the stroma and membrane fractions of chloroplasts isolated from the complemented mutant plants (Figure 2A and 2B). The global reduction of the amount of chloroplast protein complexes in *mterf9* including the plastid ribosomal protein S1 (RPS1) suggests a possible defect in chloroplast translation and ribosome biogenesis. To confirm this, we investigated the *de novo* synthesis of chloroplast proteins by leaf pulse-labeling with ^{35}S-methionine. The results showed that the synthesis rates of the RbcL and D1 chloroplast proteins were lower in *mterf9* with a respective ~50 and 80% decrease relative to WT and complemented plants, respectively (Figure 2C). Overall, the results indicated that the loss of mTERF9 activity impairs chloroplast translation.

mTERF9 deficiency causes reduced accumulation of the 16S and 23S rRNAs

Members of the mTERF family are predicted to control gene expression in organelles (Hammani et al., 2014; Kleine and Leister, 2015) and the loss of chloroplast translational activity in *mterf9* can result from the altered expression of some chloroplast genes. To identify which genes were affected in *mterf9*, we measured chloroplast gene transcripts by qRT-PCR (Figure 3) and found increased or unchanged steady-state levels of mRNAs in the *mterf9* mutant. In contrast, the 16S and 23S rRNAs were reduced compared to the WT and complemented plants. The global changes in steady-state of chloroplast mRNAs

in *mterf9* indicate that mRNA metabolism is not severely affected or presumably only secondarily affected. Therefore, these changes are unlikely to cause the reduction in the accumulation of chloroplast proteins in *mterf9*. By contrast, the observed decrease of the 16S and 23S rRNAs in *mterf9* indicate that mTERF9 is required for the accumulation of chloroplast ribosomes, which is congruent with the global reduction of chloroplast-encoded proteins in *mterf9*.

mTERF9 is required for 16S and 23S rRNA accumulations

Chloroplast rRNA genes are organized in an operon and the 16S and 23S rRNAs are co-transcribed with the 4.5S and 5S rRNAs leading to RNA precursors that are subjected to a series of processing events (reviewed in Stoppel and Meurer, 2012) (Figure 4). For example, the 23S rRNA is internally fragmented at two “hidden breaks”, leading to the accumulation of seven distinct transcripts (Figure 4A). To further investigate and confirm the decrease of the 16S and 23S rRNAs in *mterf9*, RNA gel blot analyses were conducted with probes designed to detect each rRNA and their processed forms (Figure 4B and 4C). The results confirmed the ~40% reduction in the abundance of the processed 1.5 kb 16S rRNA in *mterf9* compared to the WT or complemented plants. RNA gel blot hybridization with three probes designed to detect the different fragments of the 23S rRNA revealed a specific loss of the 2.4 kb 23S rRNA in the *mterf9* that results from the internal cleavage of the 2.9 kb 23S rRNA precursor at the first hidden break. In addition to the specific loss of the 2.4 kb processed fragment, *mterf9* showed a ~60% reduction in the level of the 2.9 kb 23S rRNA precursor compared to the WT, while the accumulation of the other fragments and the processed 4.5 and 5S rRNAs was only moderately affected. The rRNA gel blotting results confirmed the rRNA deficiencies in *mterf9* and importance of mTERF9 for the accumulation of the 16S and 23S rRNAs and the stabilization of the processed 2.4 kb 23S rRNA *in vivo*.

mTERF9 associates with the ribosomal 30S subunit to facilitate ribosomal assembly

The deficiency in the rRNAs accumulation in *mterf9* points towards a reduction in the chloroplast ribosome content in the mutant and a possible defect in ribosomal assembly.

The chloroplast 70S ribosome is composed of the small 30S and large 50S subunits that respectively contain the 16S and the 23S, 4.5S and 5S rRNAs, respectively. Preliminary immunoblotting analysis indicated a partial loss of RPS1, a protein of the 30S subunit (Figure 2A). We analyzed the sedimentation of the 30S and 50S ribosome subunits in the *mterf9*, WT and complemented plants by sucrose gradient sedimentation of stromal protein complexes (Figure 5A). The fractionation of the 30S and 50S ribosomal subunits on the gradient were monitored by immunoblotting using antibodies against RPS1 and RPL33. In the WT and complemented plants, RPL33 majorly sedimented in the last fractions of the gradient (fractions 10 to 12), whereas RPS1 sedimented in the middle of the gradient (fractions 5 to 7). By contrast, in *mterf9*, RPL33 and RPS1 sedimentation patterns were shifted to lower molecular-weight fractions with a more pronounced shifting for RPS1. These results demonstrated that the loss of mTERF9 compromised the assembly of the chloroplast ribosome subunits with a severe effect on the 30S subunit. Additional immunoblot analysis with an antibody against the Myc tag showed that mTERF9 comigrated with RPS1 indicating its primary association with the 30S ribosomal particle in chloroplasts.

We next determined whether mTERF9 associated with chloroplast ribosomes engaged in translation by polysome analysis from sucrose gradients (Figure 5B). The polysome-containing fractions were identified by immunodetection with an RPL2 antibody and by visualization of the cytosolic rRNAs by RNA electrophoresis on a denaturing agarose gel. The polysomes were detected in fractions 4 to 12 and sedimented in two groups, the light- (fractions 4 to 6) and heavy-polysomes (fractions 8 to 12). mTERF9 was detected in both the light- and heavy-polysomes as well as in the fractions of free-ribosomes (fractions 1 to 3). Treatment of the polysomes with the dissociating agent puromycin prior to their fractionation on sucrose gradient confirmed the association of mTERF9 with the polysomes as puromycin efficiently released mTERF9 from heavy to lighter complexes containing mostly monosome particles.

Altogether, the results show that mTERF9 is required for chloroplast ribosomal assembly and translation. mTERF9 primarily associates with the 30S subunit that assembles with the 50S to form the functional 70S chloroplast ribosome. In addition, its

association with the polysomes suggests that mTERF9 likely plays a role during translation.

mTERF9 binds the 16S rRNA *in vivo*

mTERF proteins are nucleic acid binding proteins that have been predominately involved in DNA-related functions in organelles. However, this perception has recently shifted with the reports of two mTERF proteins involved in RNA intron splicing in plant organelles (Hsu et al., 2014) (Hammani and Barkan, 2014). The chloroplast rRNA defects in *mterf9* and the mTERF9 association with the ribosomes suggest that this protein might bind to RNA *in vivo*. To determine whether mTERF9 binds chloroplast RNA *in vivo*, we performed genome-wide RNA co-immunoprecipitation assays (RIP). Stromal extracts from the complemented and WT plants were subjected to immunoprecipitation with antibodies raised against the Myc tag and co-immunoprecipitated RNAs were identified by hybridization to tiling microarrays of the Arabidopsis chloroplast genome (RIP-chip) (Figure 6A and 6B). The results revealed a prominently enriched peak (>20-fold) in the mTERF9 immunoprecipitate that corresponds to the 16S rRNA and to a lesser extent to the 23S, 4.5S, and 5S rRNAs. Three additional RNAs of *atpH*, *psbC* and *psbE* genes were weakly enriched (<10-fold) in the mTERF9 immunoprecipitate (Figure 6B). To quantify mTERF9 binding to the 16S and 23S rRNAs, we conducted an independent RIP experiment followed by qRT-PCR analysis of the immunoprecipitated RNAs (Figure 6C). The results showed that mTERF9 bound 10% of the 16S rRNAs from the input and only less than 2% of the 23S rRNA (Figure 6C). Finally, we performed a third RIP experiment and analyzed the immunoprecipitated RNAs by slot-blot hybridization (Figure 6D). The results indicated a strong enrichment of the 16S rRNA in mTERF9 immunoprecipitate and a weaker enrichment of the 23S and 5S rRNAs. However, the slot-blotting analysis did not validate the *psbE* RNA as an mTERF9 interactant, and was considered as a false positive target together with *atpH* and *psbC* which gave enrichment peaks of similar magnitude in the RIP-chip assay. Taken together, the results confirmed that mTERF9 primarily binds the 16S rRNA *in vivo*, which is consistent with its association with the small 30S ribosomal subunit.

The mTERF9 protein interactome confirms its link to ribosome biogenesis.

Our data demonstrated that mTERF9 is involved in ribosomal assembly and chloroplast translation. The recruitment of components of the ribosome biogenesis machinery to the 16S rRNA may be one of the key functions of an rRNA-interacting protein. To understand the protein interactome of mTERF9 *in vivo*, we performed co-immunoprecipitation of untreated or RNase-treated stromal extracts in biological triplicates and, proteins from the immunoprecipitated fractions were identified by LC-MS/MS. The efficiency of mTERF9-Myc immunoprecipitation between the RNase-treated or untreated samples was similar, allowing a direct comparison of the results (Figure 7A). We identified 158 and 173 proteins significantly enriched by mTERF9-Myc precipitation (Log2(FC)>2 and adj_*P*<0.05) in the -RNase and +RNase condition, respectively (Figure 7B and 7C). The enriched mTERF9-interacting proteins were classified in 7 groups according to their functional annotations: ribosomal proteins of the small and large subunits (SSU and LSU), CPN60 chaperonins, rRNA processing/ translation factors, RNA binding proteins (RBPs), components of the transcriptional active chromosome (TACs) and finally, the category “others” grouping chloroplast proteins with functions unrelated to gene expression and cytosolic protein contaminants (Figure 7C; Supplemental Data Set 1). Gene ontology term enrichment analyses revealed that the RNA-dependent and -independent protein interactants share over-represented molecular functions in ribosome biogenesis (Figure 7D). As an illustration, the *in vivo* fishing of mTERF9 in the absence of RNase treatment pulled down 20 out of the 24 proteins that constitute the small ribosome subunit and 27 out of the 33 ribosomal proteins composing the large subunit of chloroplasts (Tiller and Bock, 2014). Nevertheless, the RNase treatment had differential effects on the accumulation of proteins in mTERF9 co-immunoprecipitates. The treatment reduced the number of chloroplast ribosomal proteins and in particular of the large subunit, rRNA processing/translation factors and TAC components, while it increased the number of RNA binding proteins and proteins from the category “others” (Figure 7C). On contrary, all 6 subunits (CPN60α1-2, CPN60β1-4) of the chloroplast CPN60 chaperonin complex (Zhang et al., 2016) were constantly retrieved in both conditions as most enriched proteins in mTERF9 co-immunoprecipitates (Figure 6B and 6E). In total, 92 proteins were commonly found in the untreated and RNase-treated co-immunoprecipitates (Figure 6E) suggesting that the

majority of the mTERF9 interactants were not RNA-dependent but rather direct protein interactors. However, this does not exclude the possibility that the remaining co-immunoprecipitated proteins engaged in direct protein-protein interactions with mTERF9. Among the 92 common proteins, none were chloroplast RNA binding proteins, indicating that the RNase treatment efficiently destabilized ribonucleoprotein complexes and that their interaction with mTERF9 was RNA-dependent. Twelve proteins from the small and large ribosomal subunits were respectively enriched under both conditions along with 6 chloroplast rRNA processing and translation factors (Figure 6E and Supplemental Data Set 1). These include the following rRNA processing factors: RNA helicases, RH3 (Asakura et al., 2012; Lee et al., 2013) and ISE2 (Bobik et al., 2017), Ribonuclease J RNJ (Sharwood et al., 2011), RNA binding protein RHON1 (Stoppel et al., 2012) and the translation initiation and elongation factors FUG1 (Miura et al., 2007) and EF-Tu/SVR11 (Liu et al., 2019), respectively. Finally, ten TAC components co-immunoprecipitated with mTERF9 under both conditions. The TACs enrichment in mTERF9 co-immunoprecipitates was consistent with their co-localization to the nucleoids, a site known to play a major function in rRNA processing and ribosome assembly in chloroplasts (Majeran et al., 2012; Kleinknecht et al., 2014; Hotto et al., 2015). Interestingly, some ribosomal proteins, rRNA processing factors and RNA binding proteins were exclusively co-immunoprecipitated with mTERF9 by RNase treatment (Figure 7E and Supplemental Data Set 1). The RNase-dependency of these interactors revealed that their interaction with mTERF9 occurred upon mTERF9 dissociation from ribosomal nucleoprotein complexes which suggests that mTERF9 can interact with ribosomal proteins and rRNA processing factors in a spatial and sequential order during the disassembly of the ribosome subunits *in vivo*.

To validate the mTERF9 interactome and its link with ribosome biogenesis, we performed immunoblot analyses of untreated mTERF9 co-immunoprecipitates and confirmed the mTERF9 interaction with RH3, a DEAD box RNA helicase involved in rRNA processing (Asakura et al., 2012) and RPL33 and RPS1, two proteins of the large and small ribosome subunits, respectively.

In summary, the mTERF9 protein interactome was in agreement with the function of mTERF9 in chloroplast ribosome assembly. Moreover, the results showed that mTERF9 protein supports protein-protein interaction during ribosome assembly besides

its association with the 16S rRNA. Finally, the striking interaction of CPN60 chaperonins with mTERF9 *in vivo* points towards the potential implication of the CPN60 complex in chloroplast translation.

mTERF9 supports direct protein-protein interactions

mTERF-repeat proteins are considered to be putative nucleic acid binders and we indeed showed that mTERF9 interacts with the 16S rRNA *in vivo*. However, our co-immunoprecipitation assays showed that mTERF9 additionally interacts *in vivo* with many proteins that are involved in chloroplast ribosome biogenesis including, ribosomal proteins, rRNA processing factors, and unexpected chaperonins from the CPN60 family. Some of these interactions appeared to be RNase insensitive indicating that mTERF9 could support direct protein-protein interaction. To test this possibility, we used mTERF9 as a bait in a modified yeast two-hybrid assay based on split-ubiquitin, called “DUAL hunter” (Möckli et al., 2008). As mTERF9 and many ribosomal proteins partially associate to chloroplast membranes (Figure 2B) (Yamamoto et al., 1981; Hristou et al., 2019), this system offered the flexibility to select both membrane and cytosolic protein interactions. We tested the physical interaction of mTERF9 with 12 protein candidates that co-immunoprecipitated with mTERF9 in the -RNase or +RNase condition only or in both conditions (Figure 8 and Supplemental Table 1). Out of the 12 candidates tested, mTERF9 interacted with 5 proteins in yeast. These included ERA1, the Arabidopsis ortholog of the bacterial YqeH/ERA assembly factor for the 30S ribosomal subunit (Sayed et al., 1999; Loh et al., 2007), PSRP2 and RPL1, two proteins of the 30S and 50S ribosomal subunits (Graf et al., 2017), respectively, and finally, CPN60β1 and β3, two subunits of the CPN60 chaperonin complex (Zhao and Liu, 2017). These results demonstrated that mTERF9 can directly interact with ribosomal proteins from the 30S and 50S subunit, a putative 30S subunit assembly factor and CPN60 chaperonins. The facts that mTERF9 interacts physically with ERA1, a protein that was specifically co-immunoprecipitated by the RNase treatment and with PSRP2 and RPL1 whose *in vivo* association with mTERF9 was rather sensitive to RNase, reinforced the notion that mTERF9 is likely to sequentially engage in various protein interactions during chloroplast ribosomal assembly and that the rRNAs likely stabilize some of these interactions. The physical interactions between mTERF9

and CPN60 chaperonins revealed that mTERF9 might be a substrate of the CPN60 complex. Alternatively, mTERF9 might recruit the CPN60 complex to ribosomal complexes to assist folding of ribosomal proteins during subunits assembly or neosynthesized proteins during translation. Finally, we demonstrated that mTERF9 had the capacity to self-interact in yeast and that the protein oligomerization was dependent on the mTERF repeats since their truncation abolished the interaction (Figure 8B).

DISCUSSION

mTERF9 assists chloroplast ribosome assembly via ribonucleoprotein interactions

We demonstrated in this study that mTERF9/TWIRT1, a member of the mTERF family of transcriptional factors in Arabidopsis has an unexpected function in chloroplast ribosome biogenesis and translation. Our study extends the current functional repertoire of mTERF proteins in plants in a process unrelated to DNA metabolism. We found that the *mterf9* knock-out line is defective in chloroplast translation as a result of the reduced accumulation of the 16S and 23S rRNAs, two scaffolding components of the 30S small and 50S large subunits of the chloroplast ribosome, respectively. The decrease of these rRNAs is intricately linked to a lack of assembly of subunits into functional chloroplast 70S ribosomes in *mterf9*. In fact, similar to bacteria, ribosome assembly in chloroplasts is tightly connected to the post-transcriptional maturation of rRNAs (Shajani et al., 2011). For example, the orchestrated assembly of the 50S ribosomal proteins on the 23S rRNA precursor in plants is believed to expose the RNA to endonucleases at particular cleavage sites and to generate the two hidden breaks in the 23S rRNA. In *mterf9,* the stability of the first-hidden break processed 2.4 kb 23S rRNA was specifically impaired. However, the 1.3 kb 23S rRNA that results as well from processing at this site accumulated to normal level in the mutant arguing that mTERF9 is not essential for the generation of the first hidden break in the 23S rRNA but rather for the stabilization of the 2.4 kb isoform and its protection from internal cleavage at the second hidden break site. Several auxiliary factors involved in chloroplast ribosomal assembly have been recently characterized and the majority of these are bacterial homologs or harbor RNA binding domains that are conserved in bacteria (Nishimura et al., 2010; Sharwood et al., 2011; Asakura et al., 2012; Stoppel et al., 2012; Lee et al., 2013; Hotto et al., 2015; Liu et al., 2015; Bobik et al., 2017;

Zou et al., 2020). Without any surprise, these protein homologs perform conserved functions in rRNA processing and therefore, ribosome assembly in chloroplasts. On the contrary, mTERF9 belongs to a eukaryote-specific transcription factors family and its function in chloroplast ribosome assembly was unexpected. We showed that mTERF9 function relied on the contribution of two potent biochemical properties that are intrinsically linked to α-helices structures: the capacity to interact with proteins and/or nucleic acids (reviewed in Grove et al., 2008; Rubinson and Eichman, 2012). In fact, our co-immunoprecipitation analyses demonstrated that mTERF9 binds to the 16S rRNA *in vivo* as well as ribosomal proteins, CPN60 chaperonins and known auxiliary ribosomal factors involved in rRNA processing such as MraW-like 16S rRNA methyltransferase (CMAL) (Zou et al., 2020), YbeY endoribonuclease (Liu et al., 2015), RNase J (Sharwood et al., 2011), RNase E-like protein (RHON1) (Stoppel et al., 2012) or DEAD/DEAH-box RNA helicases (RH3 and ISE2) (Asakura et al., 2012; Lee et al., 2013; Bobik et al., 2017). The fractionation of chloroplast high-molecular-weight protein complexes combined with the comparative mTERF9 protein interactome in presence or absence of RNase together with the 16S rRNA mTERF9 co-immunoprecipitation indicate that mTERF9 preferentially associates with the 30S small ribosome subunit *in vivo*. We showed that some mTERF9 protein interactions were RNA independent *in vivo* and could be reconstituted in a yeast two hybrid assay, demonstrating that mTERF9 supports direct interactions with ribosomal proteins. The ability of mTERF9 to stabilize ribonucleoprotein complexes via physical interactions certainly accounts for its function in the assembly of ribosomal subunits assembly. In addition, the capacity of mTERF9 to oligomerize via intermolecular interactions between the mTERF repeats likely confers the protein new opportunities for ligand association by extending the binding surfaces at the dimer (Figure 8B). Although our results showed that mTERF9 preferentially associates with the small ribosome subunit *in vivo*, the mTERF9 protein-interactome in chloroplasts and the defect in the 23S rRNA processing that was observed in *mterf9* point towards its additional contribution in the assembly of the 50S subunit. Finally, the mTERF9 association with the polysomes indicates that it plays a function in chloroplast translation but how it participates in this process remains elusive at this stage (one possibility is discussed below).

ERA1 and CPN60 chaperonins associate to chloroplast ribosomes *in vivo*

Our work revealed the presence of proteins in mTERF9 co-immunoprecipitates whose interaction with the chloroplast ribosomes had not been reported so far. The Arabidopsis protein ERA1 has been named after its bacterial homolog, the GTP-binding ERA protein. The protein localizes to the chloroplast nucleoids (Suwastika et al., 2014) and was found in stromal megadalton complexes containing ribosomal proteins (Olinares et al., 2010) but its function has never been investigated in plants. In bacteria, the ERA1 homolog associates with the ribosome and binds the 16S rRNA to promote the assembly of the small 30S subunit (Sayed et al., 1999; Loh et al., 2007). Our results confirmed the physical interaction of Arabidopsis ERA1 with mTERF9, a protein involved in the assembly of the 30S ribosomal subunit and therefore, its likely conserved function in ribosome assembly in chloroplasts.

Another surprise in the composition of the mTERF9 protein interactome is the high-enrichment of the six subunits of the multi-subunit CPN60 chaperonin complex, which is related to the bacterial GroEL protein folding machine and has been proposed to share a conserved function in protein quality control in chloroplasts by preventing aberrant protein folding and aggregation during their import into chloroplast or during their synthesis in chloroplasts (Zhao and Liu, 2017). However, the evidence for such function in plants is scare and very few ligands of the CPN60 chaperonins have been reported so far. These include the large subunit of Rubisco, RbcL (Barraclough and Ellis, 1980), the Ferredoxin NADP+ reductase, FNR (Tsugeki and Nishimura, 1993), the NdhH subunit of the NADH dehydrogenase complex (Peng et al., 2011) and the membrane-bound FTSH11 protease (Adam et al., 2019). By confirming the *in vivo* association of the CPN60 complex with the chloroplast ribosomes and the direct interaction of CPN60β1 and β3 subunits with mTERF9, our study provides insights into the molecular function of these chaperonins in chloroplast translation. Based on the mTERF9 protein interactome and mTERF9's *in vivo* function, we propose the CPN60 chaperonin complex to be involved in the folding of nascent chloroplast proteins during translation, which would be in agreement with the chaperonin paradigm (Zhao and Liu, 2017). In this model, mTERF9 would serve as a platform for recruiting the CPN60 chaperonin complex to the chloroplast ribosomes during translation via direct protein-protein interactions. This assumption is tempting as it would

explain the functional association of mTERF9 with the chloroplast polysomes besides its role in ribosome assembly. Alternatively, the physical interaction between mTERF9 and the CPN60 complex might reflect the direct involvement of CPN60 chaperonins in the folding of mTERF9 and/or ribosomal proteins during ribosome assembly. In this scenario, the CPN60 complex would alternatively play a direct role in chloroplast ribosome biogenesis and translation. This possibility has been foreshadowed in an early study that identified nuclear mutants of maize displaying defects in the assembly of chloroplast polysomes (Barkan, 1993). The results showed that the product of a nuclear gene, *CPS2* facilitated the translation of various chloroplast mRNAs and the gene was later identified to be the maize orthologous *CPN60α1* gene, suggesting the implication of CPN60 chaperonins in translation (Belcher et al., 2015).

mTERF9 as regulator of abiotic stress responses in plants

Intriguingly, the *mterf9* allele used in this study was initially reported to exhibit altered response to various abiotic stress including salt, sugar and ABA (Robles et al., 2015). In addition, *mTERF9* was integrated into the chloroplast retrograde signaling network (Nunez-Delegido et al., 2019). Nevertheless, the *in vivo* molecular function of mTERF9 was not further studied. Our study demonstrated that mTERF9 functions in chloroplasts as a ribosomal assembly factor and its loss of function in Arabidopsis leads to reduced chloroplast translation. This suggests that the dysfunction of plastid translation likely account for *mterf9* resistance to high salinity. Many nuclear genes encoding chloroplast-localized proteins have been shown to respond to high salinity in plants (reviewed in Suo et al., 2017; Xu et al., 2017) and like *mTERF9*, some of these genes participate in chloroplast translation. For example, the reduction of chloroplast protein synthesis in the RNA helicase mutant *rh3* has been tighten to salt resistance in Arabidopsis (Gu et al., 2014). The link between reduced chloroplast protein synthesis and salt tolerance has additionally been suggested in pea by the downregulation of the chloroplast translation elongation factor *EF-Tu* in response to high salinity (Singh et al., 2004). Both, the RH3 and Arabidopsis ortholog EF-Tu/SVR11 proteins physically interact with mTERF9 *in vivo*. However, how the decrease in chloroplast protein synthesis in these mutants feeds the stress-response pathway in plants remains to be elucidated.

METHODS

Oligonucleotides used in this study are listed in Supplemental Data Set 2.

Plant material

Arabidopsis thaliana ecotype Columbia (Col-0) and *Nicotania benthamiana* were used in this study. The T-DNA insertion mutant allele *mterf9* (WiscDsLox474E07) was obtained from the ABRC Stock Center. Complemented mutants were obtained via *Agrobacterium tumefaciens* transformation of *mterf9* homozygous plants. The binary vector (pGWB17) used for agro-transformation expressed the At5g55580 coding sequence in fusion with a 4xMyc C-terminal tag under the control of the CaMV 35S promoter. Transgenic plants were selected on Murashige and Skoog (MS) plates containing 25 μg/mL hygromycin. Experiments were performed using 7-day-old plants grown *in vitro* (1× MS pH5.7, 0.5% sucrose, 0.8% Agar; 16 h light: 8 h dark cycles; 65-85 μmol photons m^{-2} s^{-1}), 14-day-old plants grown on soil for chloroplast isolation or 4-week-old plants for protein pulse labelling experiments.

Subcellular localization of mTERF9

Nicotiana benthamiana leaves were infiltrated with *Agrobacterium tumefaciens* GV3101 carrying pMDC83*:mTERF9* and pB7RWG2*:RAP* at an OD_{600} of 0.5 each. Protoplasts were prepared as described previously (Berglund et al., 2009) and examined under a Zeiss LSM 780 confocal microscope. GFP was excited at 488 nm and emission was acquired between 493-556 nm. RFP and chlorophyll were excited at 561 nm and emissions were acquired between 588-641 nm and 671-754 nm, respectively.

Chlorophyll a fluorescence induction and light-Induced PSI absorbance changes

Chlorophyll *a* fluorescence induction kinetics and PSI absorbance changes at 820 nm were performed with leaves of 2-week-old WT, *mterf9* mutant and complemented mutant plants grown on soil using a Dual-PAM-100 System (Walz, Effeltrich, Germany) (Meurer et al., 1996). Φ_{PSI}, $\Phi_{PSI\ NA}$ and $\Phi_{PSI\ ND}$ were expressed as described (Klughammer and Schreiber, 1994).

RNA extraction and analyses

Tissues were ground in liquid nitrogen and RNA was extracted with Trizol following manufacturer's protocol (Invitrogen™). RNA was further extracted with phenol-chloroform pH 4.3. Five μg of Turbo DNase (Thermo Fisher) treated RNAs were used for Superscript IV reverse transcription with random hexamers. The resulting cDNA was diluted 20-fold for qPCR reaction. *ACT2 (AT3G18780)* and *TIP41 (AT1G13440)* were used as reference genes. For RNA gel blotting, 0.5 μg of RNA was fractionated on 1.2% agarose-1% formaldehyde gel and blotted as described (Barkan, 1998). Gene PCR products of 200-300 bp were labelled with ^{32}P-dCTP following the prime-a-gene labelling kit instructions (Promega) and used as probes (Supplemental Data Set 2). Results were visualized on an Amersham Typhoon imager and data quantification was performed with ImageJ.

Protein analyses

For *in vivo* labeling of chloroplast proteins, leaf discs of *Arabidopsis* plants were incubated in 1 mM K_2HPO_4/KH_2PO_4 pH 6.3, 1% Tween-20, 20 μg/mL cycloheximide, 100 μCi ^{35}S-methionine and vacuum infiltrated. Leaf discs were kept under light for 15 min, washed in water and frozen in liquid nitrogen. Proteins were extracted in Tris pH 7.5, 10% glycerol, 1% NP40, 5 mM EDTA, 2 mM EGTA, 35 mM β-mercaptoethanol, 1× EDTA-free protease inhibitor cocktail (Roche), and 200,000 cpm per sample were resolved on SDS-PAGE. After electrophoresis, the gel was stained in 50% methanol, 10% glacial acetic acid, 0.5 g/l Coomassie brilliant blue R-250 and vacuum dried before being exposed to a phosphimager plate. Results were visualized on an Amersham Typhoon imager. For immunoblot analysis, total leaf proteins were extracted in the same buffer, resolved on SDS-PAGE and transferred onto PVDF membrane at 80 V for 1,5 h using the wet transfer. Anti-PsaD, -PetD and -RH3 antibodies were donations of Alice Barkan (University of Oregon). Anti-NdhL, -NdhB and -RbcL antibodies were donations of Toshiharu Shikanai (University of Kyoto) and Géraldine Bonnard (CNRS UPR2357), respectively. Other antibodies against chloroplast proteins were purchased from Agrisera and anti-Myc antibodies (clone 9E10) from Sigma-Aldrich.

527 **Chloroplast isolation and fractionation**

528 Chloroplasts were purified by density gradient and differential centrifugations as described
529 previously (Kunst, 1998). Chloroplasts were lysed in 30 mM Hepes-KOH pH 8, 10 mM
530 MgOAc, 60 mM KOAc, 1 mM DTT, 1× EDTA-free protease inhibitor cocktail and 1 mM
531 PMSF. Stromal (soluble) and thylakoid proteins were separated by centrifugation at
532 20,000 g for 10 min at 4°C.

533

534 **Sucrose gradient fractionation**

535 For the analysis of high-molecular-weight complexes by differential sedimentation, 0.25
536 mg of stromal proteins were fractionated on 10-30% linear sucrose gradient at 235,000 g
537 for 4 hours at 4°C. Polysome analyses were performed on leaf tissues as described
538 (Barkan, 1998).

539

540 **CoIP-MS**

541 Two mg of stromal proteins treated or not with 100 μg/mL RNase A and 250 U/mL RNase
542 T1 mix (Thermo Fisher) were diluted in one volume of Co-IP buffer (20 mM Tris pH 7.5,
543 150 mM NaCl, 15 mM $MgCl_2$, 0.5 mM DTT, 3mM ATP, 1 mM EDTA, 1% NP-40, 1× EDTA-
544 free protease inhibitor cocktail, 1 mM PMSF) and incubated with 50 μL of anti-MYC
545 Miltenyi magnetic beads at 4°C for 30 min on a rotator. Beads were washed in Co-IP
546 buffer and eluted as recommended by the manufacturer. Eluted proteins were prepared
547 as described (Chicher et al., 2015; Méteignier et al., 2020). Briefly, proteins were
548 precipitated overnight with 5 volumes of cold 0.1 M ammonium acetate in 100% methanol
549 and digested with sequencing-grade trypsin (Promega) and each sample was analyzed
550 by nanoLC-MS/MS on a QExactive+ mass spectrometer coupled to an EASY-nanoLC-
551 1000 (Thermo Fisher). Data were searched against the *Arabidopsis thaliana* TAIR
552 database with a decoy strategy (release TAIRv10, 27282 forward protein sequences).
553 Peptides and proteins were identified with Mascot algorithm (version 2.5.1, Matrix
554 Science, London, UK) and data were further imported into Proline v1.4 software
555 (http://proline.profiproteomics.fr/). Proteins were validated on Mascot pretty rank equal to
556 1, and 1% FDR on both peptide spectrum matches (PSM score) and protein sets (Protein
557 Set score). The total number of MS/MS fragmentation spectra was used to relatively

quantify each protein (Spectral Count relative quantification). Proline was further used to align the Spectral Count values across all samples. The mass spectrometrics data were deposited to the ProteomeXchange Consortium via the PRIDE partner repository (Perez-Riverol et al., 2019) with the dataset identifier PXD018987 and 10.6019/PXD018987.

For the statistical analysis of the co-immunoprecipitation proteomes, the mass-spectrometry data collected from three biological replicates of the experimental mTERF-Myc coIPs were compared to biological triplicates of control WT coIPs using RStudio v1.1.456 and the R package IPinquiry v1.2. The size factors used to scale samples were calculated according to the DESeq2 normalisation method (Anders and Huber, 2010). EdgeR v3.14.0 and Stats v3.3.1 were used to perform a negative binomial test and calculate the fold changes and adjusted *P*-values corrected by Benjamini–Hochberg for each identified protein. The $-\log_{10}$ (adj_*P*) and volcano plot graphs were calculated and drawn with Excel, respectively. The functional protein annotations were retrieved from the TAIR database (Lamesch et al., 2012) using the bulk data retrieval tool. The complete list of protein interactants and the number of peptides are provided in Supplemental Data Set 1.

Yeast two hybrid analysis

Coding sequences of *mTERF9* or putative interacting partners were cloned into the bait vector pDHB1 or prey vector pPR3-N (DualsystemsBiotech)(Möckli et al., 2008). The NMYZ51 yeast strain was co-transformed with bait and prey vectors using the PEG/LiOAc method (Gietz and Schiestl, 2007). Co-transformants were selected on yeast synthetic and drop-out (DO) minus leucine (L) and tryptophan (W) agar medium. Positive colonies were sub-cultured in -WL DO liquid medium overnight. Overnight cultures were diluted to an OD_{600} of 0.3 to make the starting cultures and diluted by tenfolds to 10^{-2}. Five µL of each dilution was plated on -WL DO agar medium or on DO medium minus leucine, tryptophan, histidine and adenine (-WLHA) supplemented with 3-aminotriazol to select protein interactions. 3-AT was used at concentrations of 1 mM to test mTERF9 interaction with ERA1 and mTERF9, 2 mM with PSRP2 and RPL1 and 40 mM for CPNB1 and CPNB3.

589 **RNA immunopurification analysis**

590 0.5 mg of stromal proteins were diluted in 450 µL of RIP buffer (20 mM Tris pH 7.5, 150
591 mM NaCl, 1 mM EDTA, 1% NP-40, 1× EDTA-free protease inhibitor cocktail, 1 mM PMSF)
592 and incubated with 50 µL of anti-MYC Miltenyi magnetic beads at 4°C for 30 min on a
593 rotator. Beads were washed and eluted in RIP buffer supplemented with 1% SDS.
594 Immunoprecipitated and supernatant RNAs were extracted with Trizol and further purified
595 with phenol/chloroform. The RNA from the pellet and 3.5 µg RNA from the supernatant
596 were fragmented and labelled with Cy5 (635 nm) and Cy3 (532 nm), respectively and
597 hybridized on a tilling microarray (chip) covering the Arabidopsis chloroplast genome, as
598 described in (Trosch et al., 2018). Data were analyzed with GenePix Pro 7.0 software with
599 local background subtraction method. The median of ratios of the background-subtracted
600 pellet to supernatant signals were calculated and the super-ratios of the mTERF9 IP to
601 control IP were plotted along the Arabidopsis chloroplast genome. RIP-chip data are
602 provided in Supplemental Data Set 3.

603 For the slot-blot hybridization analysis, half of the IP RNA and one twentieth of the
604 supernatant RNA were applied to a nylon membrane with a slot-blot manifold and
605 hybridized to radiolabeled gene probes as described (Ostheimer et al., 2003). For qRT-
606 PCR analysis, half of the input and IP RNAs were treated with Turbo DNase (Thermo
607 Fisher) and cDNA synthesis and qPCR were conducted as described above.

608

609 **Accession numbers**

610 The gene described in this article corresponds to the following Arabidopsis Genome
611 Initiative code: At5g55580 (mTERF9). AGI codes of mTERF9 protein interactors can be
612 found in Supplemental Data Set 1. The T-DNA mutant used was WiscDsLox474E07
613 (*mterf9*).

614

615 **Supplemental Data**

616 **Supplemental Table 1.** List of prey proteins tested in the yeast-two hybrid assay.

617 **Supplemental Data Set 1.** List of proteins identified by LC-MS/MS in co-
618 immunopurification assays using mTERF9 as bait.

Supplemental Data Set 2. List of oligonucleotides used in this study.

Supplemental Data Set 3. RIP-Chip data showing enrichment of RNA Sequences in mTERF9 immunoprecipitations.

ACKNOWLEDGMENTS

This study was supported by a grant from Agence Nationale de la Recherche (ANR-16-CE20-0007) and the IdEx Unistra from the Investments for the future program of the French Government to KH, the DFG (ZO 302/5-1) to RZ and the SFB-TRR175 to JM (A03) and RZ (A04). The mass spectrometry instrumentation was funded by the University of Strasbourg, IdEx “Equipement mi-lourd” 2015.

AUTHOR CONTRIBUTIONS

KH and L-VM designed the research. L-VM, RG, KH, AZ, LK and JM performed research. KH, L-VM, RG, JC, JM and RZ analyzed the data. KH and L-VM wrote the paper and RZ, RG and JM edited it.

REFERENCES

Adam, Z., Aviv-Sharon, E., Keren-Paz, A., Naveh, L., Rozenberg, M., Savidor, A., and Chen, J. (2019). The Chloroplast Envelope Protease FTSH11 - Interaction With CPN60 and Identification of Potential Substrates. Front Plant Sci **10,** 428.

Anders, S., and Huber, W. (2010). Differential expression analysis for sequence count data. Genome Biol **11,** R106.

Asakura, Y., Galarneau, E., Watkins, K.P., Barkan, A., and van Wijk, K.J. (2012). Chloroplast RH3 DEAD box RNA helicases in maize and Arabidopsis function in splicing of specific group II introns and affect chloroplast ribosome biogenesis. Plant Physiol **159,** 961-974.

Babiychuk, E., Vandepoele, K., Wissing, J., Garcia-Diaz, M., De Rycke, R., Akbari, H., Joubes, J., Beeckman, T., Jansch, L., Frentzen, M., Van Montagu, M.C., and Kushnir, S. (2011). Plastid gene expression and plant development require a plastidic protein of the mitochondrial transcription termination factor family. Proc Natl Acad Sci U S A **108,** 6674-6679.

650 **Barkan, A.** (1993). Nuclear Mutants of Maize with Defects in Chloroplast Polysome
651 Assembly Have Altered Chloroplast RNA Metabolism. Plant Cell **5,** 389-402.
652 **Barkan, A.** (1998). Approaches to investigating nuclear genes that function in chloroplast
653 biogenesis in land plants. Method Enzymol **297,** 38-57.
654 **Barraclough, R., and Ellis, R.J.** (1980). Protein synthesis in chloroplasts. IX. Assembly
655 of newly-synthesized large subunits into ribulose bisphosphate carboxylase in
656 isolated intact pea chloroplasts. Biochim Biophys Acta **608,** 19-31.
657 **Belcher, S., Williams-Carrier, R., Stiffler, N., and Barkan, A.** (2015). Large-scale
658 genetic analysis of chloroplast biogenesis in maize. Biochim Biophys Acta **1847,**
659 1004-1016.
660 **Berglund, A.K., Pujol, C., Duchene, A.M., and Glaser, E.** (2009). Defining the
661 determinants for dual targeting of amino acyl-tRNA synthetases to mitochondria
662 and chloroplasts. J Mol Biol **393,** 803-814.
663 **Bobik, K., McCray, T.N., Ernest, B., Fernandez, J.C., Howell, K.A., Lane, T., Staton,**
664 **M., and Burch-Smith, T.M.** (2017). The chloroplast RNA helicase ISE2 is required
665 for multiple chloroplast RNA processing steps in Arabidopsis thaliana. Plant J **91,**
666 114-131.
667 **Bryant, N., Lloyd, J., Sweeney, C., Myouga, F., and Meinke, D.** (2011). Identification of
668 nuclear genes encoding chloroplast-localized proteins required for embryo
669 development in Arabidopsis. Plant Physiol **155,** 1678-1689.
670 **Chicher, J., Simonetti, A., Kuhn, L., Schaeffer, L., Hammann, P., Eriani, G., and**
671 **Martin, F.** (2015). Purification of mRNA-programmed translation initiation
672 complexes suitable for mass spectrometry analysis. Proteomics **15,** 2417-2425.
673 **Ding, S., Zhang, Y., Hu, Z., Huang, X., Zhang, B., Lu, Q., Wen, X., Wang, Y., and Lu,**
674 **C.** (2019). mTERF5 Acts as a Transcriptional Pausing Factor to Positively Regulate
675 Transcription of Chloroplast *psbEFLJ*. Mol Plant **12,** 1259-1277.
676 **Olinares, P.D., Ponnala, L., and van Wijk, K.J.** (2010). Megadalton complexes in the
677 chloroplast stroma of Arabidopsis thaliana characterized by size exclusion
678 chromatography, mass spectrometry, and hierarchical clustering. Mol Cell
679 Proteomics **9,** 1594-1615.

Gietz, R.D., and Schiestl, R.H. (2007). High-efficiency yeast transformation using the LiAc/SS carrier DNA/PEG method. Nature Protocols **2,** 31-34.

Graf, M., Arenz, S., Huter, P., Donhofer, A., Novacek, J., and Wilson, D.N. (2017). Cryo-EM structure of the spinach chloroplast ribosome reveals the location of plastid-specific ribosomal proteins and extensions. Nucleic Acids Res **45,** 2887-2896.

Grove, T.Z., Cortajarena, A.L., and Regan, L. (2008). Ligand binding by repeat proteins: natural and designed. Curr Opin Struct Biol **18,** 507-515.

Gu, L., Xu, T., Lee, K., Lee, K.H., and Kang, H. (2014). A chloroplast-localized DEAD-box RNA helicaseAtRH3 is essential for intron splicing and plays an important role in the growth and stress response in Arabidopsis thaliana. Plant Physiol Biochem **82,** 309-318.

Hammani, K., and Barkan, A. (2014). An mTERF domain protein functions in group II intron splicing in maize chloroplasts. Nucleic Acids Res **42,** 5033-5042.

Hammani, K., Bonnard, G., Bouchoucha, A., Gobert, A., Pinker, F., Salinas, T., and Giege, P. (2014). Helical repeats modular proteins are major players for organelle gene expression. Biochimie **100C,** 141-150.

Hotto, A.M., Castandet, B., Gilet, L., Higdon, A., Condon, C., and Stern, D.B. (2015). Arabidopsis chloroplast mini-ribonuclease III participates in rRNA maturation and intron recycling. Plant Cell **27,** 724-740.

Hristou, A., Gerlach, I., Stolle, D.S., Neumann, J., Bischoff, A., Dunschede, B., Nowaczyk, M.M., Zoschke, R., and Schunemann, D. (2019). Ribosome-Associated Chloroplast SRP54 Enables Efficient Cotranslational Membrane Insertion of Key Photosynthetic Proteins. Plant Cell **31,** 2734-2750.

Hsu, Y.W., Wang, H.J., Hsieh, M.H., Hsieh, H.L., and Jauh, G.Y. (2014). Arabidopsis mTERF15 is required for mitochondrial *nad2* intron 3 splicing and functional complex I activity. PLoS One **9,** e112360.

Huang da, W., Sherman, B.T., and Lempicki, R.A. (2009). Systematic and integrative analysis of large gene lists using DAVID bioinformatics resources. Nat Protoc **4,** 44-57.

Jimenez-Menendez, N., Fernandez-Millan, P., Rubio-Cosials, A., Arnan, C., Montoya, J., Jacobs, H.T., Bernado, P., Coll, M., Uson, I., and Sola, M. (2010). Human mitochondrial mTERF wraps around DNA through a left-handed superhelical tandem repeat. Nat Struct Mol Biol **17,** 891-893.

Kleine, T. (2012). Arabidopsis thaliana mTERF proteins: evolution and functional classification. Front Plant Sci **3,** 233.

Kleine, T., and Leister, D. (2015). Emerging functions of mammalian and plant mTERFs. Biochim Biophys Acta **1847,** 786-797.

Kleinknecht, L., Wang, F., Stube, R., Philippar, K., Nickelsen, J., and Bohne, A.V. (2014). RAP, the sole octotricopeptide repeat protein in Arabidopsis, is required for chloroplast 16S rRNA maturation. Plant Cell **26,** 777-787.

Klughammer, C., and Schreiber, U. (1994). An improved method, using saturating light pulses, for the determination of photosystem I quantum yield via P700+-absorbance changes at 830 nm. Planta **192,** 261-268.

Kunst, L. (1998). Preparation of physiologically active chloroplasts from Arabidopsis. Methods Mol Biol **82,** 43-48.

Lamesch, P., Berardini, T.Z., Li, D., Swarbreck, D., Wilks, C., Sasidharan, R., Muller, R., Dreher, K., Alexander, D.L., Garcia-Hernandez, M., Karthikeyan, A.S., Lee, C.H., Nelson, W.D., Ploetz, L., Singh, S., Wensel, A., and Huala, E. (2012). The Arabidopsis Information Resource (TAIR): improved gene annotation and new tools. Nucleic Acids Res **40,** D1202-1210.

Lee, K.H., Park, J., Williams, D.S., Xiong, Y., Hwang, I., and Kang, B.H. (2013). Defective chloroplast development inhibits maintenance of normal levels of abscisic acid in a mutant of the Arabidopsis RH3 DEAD-box protein during early post-germination growth. Plant J **73,** 720-732.

Linder, T., Park, C.B., Asin-Cayuela, J., Pellegrini, M., Larsson, N.G., Falkenberg, M., Samuelsson, T., and Gustafsson, C.M. (2005). A family of putative transcription termination factors shared amongst metazoans and plants. Curr Genet **48,** 265-269.

Liu, J., Zhou, W., Liu, G., Yang, C., Sun, Y., Wu, W., Cao, S., Wang, C., Hai, G., Wang, Z., Bock, R., Huang, J., and Cheng, Y. (2015). The conserved endoribonuclease

YbeY is required for chloroplast ribosomal RNA processing in Arabidopsis. Plant Physiol **168,** 205-221.

Liu, S., Zheng, L., Jia, J., Guo, J., Zheng, M., Zhao, J., Shao, J., Liu, X., An, L., Yu, F., and Qi, Y. (2019). Chloroplast Translation Elongation Factor EF-Tu/SVR11 Is Involved in var2-Mediated Leaf Variegation and Leaf Development in Arabidopsis. Front Plant Sci **10,** 295.

Loh, P.C., Morimoto, T., Matsuo, Y., Oshima, T., and Ogasawara, N. (2007). The GTP-binding protein YqeH participates in biogenesis of the 30S ribosome subunit in Bacillus subtilis. Genes Genet Syst **82,** 281-289.

Majeran, W., Friso, G., Asakura, Y., Qu, X., Huang, M., Ponnala, L., Watkins, K.P., Barkan, A., and van Wijk, K.J. (2012). Nucleoid-enriched proteomes in developing plastids and chloroplasts from maize leaves: a new conceptual framework for nucleoid functions. Plant Physiol **158,** 156-189.

Méteignier, L.V., Ghandour, R., Meierhoff, K., Zimmerman, A., Chicher, J., Baumberger, N., Alioua, A., Meurer, J., Zoschke, R., and Hammani, K. (2020). The Arabidopsis mTERF-repeat MDA1 protein plays a dual function in transcription and stabilization of specific chloroplast transcripts within the *psbE* and *ndhH* operons. New Phytologist **DOI:** 10.1111/nph.16625.

Meurer, J., Meierhoff, K., and Westhoff, P. (1996). Isolation of high-chlorophyll-fluorescence mutants of Arabidopsis thaliana and their characterisation by spectroscopy, immunoblotting and northern hybridisation. Planta **198,** 385-396.

Miura, E., Kato, Y., Matsushima, R., Albrecht, V., Laalami, S., and Sakamoto, W. (2007). The balance between protein synthesis and degradation in chloroplasts determines leaf variegation in Arabidopsis yellow variegated mutants. Plant Cell **19,** 1313-1328.

Möckli, N., Deplazes, A., and Auerbach, D. (2008). Finding new protein interactions using the DUALhunter system. Nature Methods **5,** i-ii.

Mokry, M., Nijman, I.J., van Dijken, A., Benjamins, R., Heidstra, R., Scheres, B., and Cuppen, E. (2011). Identification of factors required for meristem function in Arabidopsis using a novel next generation sequencing fast forward genetics approach. BMC Genomics **12,** 256.

772 **Nishimura, K., Ashida, H., Ogawa, T., and Yokota, A.** (2010). A DEAD box protein is
773 required for formation of a hidden break in Arabidopsis chloroplast 23S rRNA. Plant
774 J **63,** 766-777.
775 **Nunez-Delegido, E., Robles, P., Ferrandez-Ayela, A., and Quesada, V.** (2019).
776 Functional analysis of mTERF5 and mTERF9 contribution to salt tolerance, plastid
777 gene expression and retrograde signalling in Arabidopsis thaliana. Plant Biol
778 (Stuttg) **DOI:** 10.1111/plb.13084
779 **Ostheimer, G.J., Williams-Carrier, R., Belcher, S., Osborne, E., Gierke, J., and**
780 **Barkan, A.** (2003). Group II intron splicing factors derived by diversification of an
781 ancient RNA-binding domain. EMBO J **22,** 3919-3929.
782 **Peng, L., Fukao, Y., Myouga, F., Motohashi, R., Shinozaki, K., and Shikanai, T.**
783 (2011). A chaperonin subunit with unique structures is essential for folding of a
784 specific substrate. PLoS Biol **9,** e1001040.
785 **Perez-Riverol, Y., Csordas, A., Bai, J., Bernal-Llinares, M., Hewapathirana, S.,**
786 **Kundu, D.J., Inuganti, A., Griss, J., Mayer, G., Eisenacher, M., Perez, E.,**
787 **Uszkoreit, J., Pfeuffer, J., Sachsenberg, T., Yilmaz, S., Tiwary, S., Cox, J.,**
788 **Audain, E., Walzer, M., Jarnuczak, A.F., Ternent, T., Brazma, A., and Vizcaino,**
789 **J.A.** (2019). The PRIDE database and related tools and resources in 2019:
790 improving support for quantification data. Nucleic Acids Res **47,** D442-D450.
791 **Robles, P., Micol, J.L., and Quesada, V.** (2015). Mutations in the plant-conserved
792 MTERF9 alter chloroplast gene expression, development and tolerance to abiotic
793 stress in Arabidopsis thaliana. Physiol Plant **154,** 297-313.
794 **Robles, P., Navarro-Cartagena, S., Ferrandez-Ayela, A., Nunez-Delegido, E., and**
795 **Quesada, V.** (2018). The Characterization of Arabidopsis mterf6 Mutants Reveals
796 a New Role for mTERF6 in Tolerance to Abiotic Stress. Int J Mol Sci **19**.
797 **Romani, I., Manavski, N., Morosetti, A., Tadini, L., Maier, S., Kuhn, K., Ruwe, H.,**
798 **Schmitz-Linneweber, C., Wanner, G., Leister, D., and Kleine, T.** (2015). A
799 Member of the Arabidopsis Mitochondrial Transcription Termination Factor Family
800 Is Required for Maturation of Chloroplast Transfer RNAIle(GAU). Plant Physiol **169,**
801 627-646.

802 **Rubinson, E.H., and Eichman, B.F.** (2012). Nucleic acid recognition by tandem helical
803 repeats. Curr Opin Struct Biol **22,** 101-109.
804 **Sayed, A., Matsuyama, S., and Inouye, M.** (1999). Era, an essential Escherichia coli
805 small G-protein, binds to the 30S ribosomal subunit. Biochem Biophys Res
806 Commun **264,** 51-54.
807 **Shajani, Z., Sykes, M.T., and Williamson, J.R.** (2011). Assembly of bacterial ribosomes.
808 Annu Rev Biochem **80,** 501-526.
809 **Sharwood, R.E., Halpert, M., Luro, S., Schuster, G., and Stern, D.B.** (2011).
810 Chloroplast RNase J compensates for inefficient transcription termination by
811 removal of antisense RNA. RNA **17,** 2165-2176.
812 **Singh, B.N., Mishra, R.N., Agarwal, P.K., Goswami, M., Nair, S., Sopory, S.K., and**
813 **Reddy, M.K.** (2004). A pea chloroplast translation elongation factor that is
814 regulated by abiotic factors. Biochem Biophys Res Commun **320,** 523-530.
815 **Spahr, H., Samuelsson, T., Hallberg, B.M., and Gustafsson, C.M.** (2010). Structure of
816 mitochondrial transcription termination factor 3 reveals a novel nucleic acid-binding
817 domain. Biochem Biophys Res Commun **397,** 386-390.
818 **Stoppel, R., and Meurer, J.** (2012). The cutting crew - ribonucleases are key players in
819 the control of plastid gene expression. J Exp Bot **63,** 1663-1673.
820 **Stoppel, R., Manavski, N., Schein, A., Schuster, G., Teubner, M., Schmitz-**
821 **Linneweber, C., and Meurer, J.** (2012). RHON1 is a novel ribonucleic acid-binding
822 protein that supports RNase E function in the Arabidopsis chloroplast. Nucleic
823 Acids Res **40,** 8593-8606.
824 **Suo, J., Zhao, Q., David, L., Chen, S., and Dai, S.** (2017). Salinity Response in
825 Chloroplasts: Insights from Gene Characterization. Int J Mol Sci **18**, 1011.
826 **Suwastika, I.N., Denawa, M., Yomogihara, S., Im, C.H., Bang, W.Y., Ohniwa, R.L.,**
827 **Bahk, J.D., Takeyasu, K., and Shiina, T.** (2014). Evidence for lateral gene transfer
828 (LGT) in the evolution of eubacteria-derived small GTPases in plant organelles.
829 Front Plant Sci **5,** 678.
830 **Tiller, N., and Bock, R.** (2014). The translational apparatus of plastids and its role in plant
831 development. Mol Plant **7,** 1105-1120.

Trosch, R., Barahimipour, R., Gao, Y., Badillo-Corona, J.A., Gotsmann, V.L., Zimmer, D., Muhlhaus, T., Zoschke, R., and Willmund, F. (2018). Commonalities and differences of chloroplast translation in a green alga and land plants. Nat Plants **4,** 564-575.

Tsugeki, R., and Nishimura, M. (1993). Interaction of homologues of Hsp70 and Cpn60 with ferredoxin-NADP+ reductase upon its import into chloroplasts. FEBS Lett **320,** 198-202.

Tzafrir, I., Pena-Muralla, R., Dickerman, A., Berg, M., Rogers, R., Hutchens, S., Sweeney, T.C., McElver, J., Aux, G., Patton, D., and Meinke, D. (2004). Identification of genes required for embryo development in Arabidopsis. Plant Physiol **135,** 1206-1220.

Xiong, H.B., Wang, J., Huang, C., Rochaix, J.D., Lin, F.M., Zhang, J.X., Ye, L.S., Shi, X.H., Yu, Q.B., and Yang, Z.N. (2020). mTERF8, a Member of the Mitochondrial Transcription Termination Factor Family, Is Involved in the Transcription Termination of Chloroplast Gene *psbJ*. Plant Physiol **182,** 408-423.

Xu, D., Leister, D., and Kleine, T. (2017). Arabidopsis thaliana mTERF10 and mTERF11, but Not mTERF12, Are Involved in the Response to Salt Stress. Front Plant Sci **8,** 1213.

Yakubovskaya, E., Mejia, E., Byrnes, J., Hambardjieva, E., and Garcia-Diaz, M. (2010). Helix unwinding and base flipping enable human MTERF1 to terminate mitochondrial transcription. Cell **141,** 982-993.

Yamamoto, T., Burke, J., Autz, G., and Jagendorf, A.T. (1981). Bound Ribosomes of Pea Chloroplast Thylakoid Membranes: Location and Release in Vitro by High Salt, Puromycin, and RNase. Plant Physiol **67,** 940-949.

Zhang, S., Zhou, H., Yu, F., Bai, C., Zhao, Q., He, J., and Liu, C. (2016). Structural insight into the cooperation of chloroplast chaperonin subunits. BMC Biol **14,** 29.

Zhang, Y., Cui, Y.L., Zhang, X.L., Yu, Q.B., Wang, X., Yuan, X.B., Qin, X.M., He, X.F., Huang, C., and Yang, Z.N. (2018). A nuclear-encoded protein, mTERF6, mediates transcription termination of rpoA polycistron for plastid-encoded RNA polymerase-dependent chloroplast gene expression and chloroplast development. Sci Rep **8,** 11929.

Zhao, Q., and Liu, C. (2017). Chloroplast Chaperonin: An Intricate Protein Folding Machine for Photosynthesis. Front Mol Biosci **4,** 98.

Zhao, Y., Cai, M., Zhang, X., Li, Y., Zhang, J., Zhao, H., Kong, F., Zheng, Y., and Qiu, F. (2014). Genome-wide identification, evolution and expression analysis of mTERF gene family in maize. PLoS One **9,** e94126.

Zhou, B., Zhang, L., Ullah, A., Jin, X., Yang, X., and Zhang, X. (2016). Identification of Multiple Stress Responsive Genes by Sequencing a Normalized cDNA Library from Sea-Land Cotton (Gossypium barbadense L.). PLoS One **11,** e0152927.

Zou, M., Mu, Y., Chai, X., Ouyang, M., Yu, L.J., Zhang, L., Meurer, J., and Chi, W. (2020). The critical function of the plastid rRNA methyltransferase, CMAL, in ribosome biogenesis and plant development. Nucleic Acids Res **48,** 3195-3210.

FIGURE LEGENDS

Figure 1. mTERF9 is a chloroplast nucleoid-associated protein required for plant development. (A) Schematic representation of the *mTERF9* gene and protein with the position of the *mterf9* T-DNA insertion. **(B)** Phenotypes of wild-type (WT), *mterf9* and complemented (CP) plants grown in medium or soil at indicated growth stages. **(C)** RT-PCR analysis of *mTERF9* expression in WT, *mterf9* and complemented plants. Genomic DNA (gDNA) was used as positive control for PCR and *ACTIN-2 ACT2* serves as internal control for RT-PCR. **(D)** Subcellular localization of mTERF9-GFP and RAP-GFP fusion proteins in tobacco leaf protoplasts. Close-up views of the framed area are shown below. Scale bar: 5 μm.

Figure 2. Chloroplast protein accumulation deficiency in *mterf9*. (A) Immunoblot analyses of total leaf protein extracts with antibodies against mTERF9-Myc and subunits of the photosystem I (PsaD), photosystem II (PsbD, PsbH, PsbE,), Cytochrome b_6f (PetD), NADH dehydrogenase (NdhB, NdhL), ATP synthase (AtpA), Rubisco (RbcL), light-harvesting complex II (LHCB2) and ribosome (RPS1) complexes. Replicate membranes were stained with Coomassie Blue (CBB) to show equal protein loading. **(B)** mTERF9 localizes to the stroma and chloroplast membranes. Isolated chloroplasts were lysed in hypotonic buffer and membrane and soluble protein fractions were separated by

894 centrifugation. Chloroplast (C), soluble (S), and membrane (M) protein fractions were
895 analyzed by immunoblotting using antibodies against Myc epitope, a stromal protein
896 (Fructose-bisphosphate aldolase 1) and a membrane associated subunit of the ATP
897 synthase complex (AtpA). The Coomassie Blue (CBB) stained membrane is shown. **(C)**
898 *In vivo* chloroplast translation assays. Leaf discs from the indicated genotypes were
899 pulsed-labelled with ^{35}S-Methionine and neosynthesized proteins were separated by
900 SDS-PAGE and visualized by autoradiography. The CBB stained gel is shown below and
901 serves as equal loading control.
902
903 **Figure 3. Steady state levels of chloroplast gene transcripts in Arabidopsis in**
904 ***mterf9* and CP plants.** Transcript levels were determined by qRT-PCR and are displayed
905 as the $\log_2$ fold change (FC) between values obtained for the mutant or the complemented
906 plants and the WT plants. Genes are ordered according to their genome positions. The
907 nuclear *ACT2* and *TIP41* genes were used for data normalization. The values from two
908 biological replicates performed each with technical triplicate were averaged per genotype
909 and standard errors are indicated.
910
911 **Figure 4. Defects in the 16S and 23S rRNA accumulation in *mterf9* plants. (A)**
912 Schematic representation of the chloroplast rRNA operon. Exons and introns are
913 represented by gray and white boxes, respectively. The positions of the probes used for
914 RNA blot hybridization are indicated beneath the map. The *23S* rRNA hidden breaks
915 positions are shown above the gene with black arrowheads. The major accumulating
916 transcripts for the 16S and 23S rRNA genes are mapped with arrows and their size is
917 given in kb below. Transcripts specifically impaired in the *mterf9* are indicated with
918 symbols. **(B)** Total leaf RNA (0.5 μg) was analyzed by RNA gel blot hybridization using
919 probes diagrammed in (A). **(C)** Relative quantification to wild-type (WT) in the
920 accumulation of the chloroplast rRNAs in *mterf9* and complemented (CP) plants.
921
922 **Figure 5. mTERF9 associates with chloroplast ribosomes and polysomes *in vivo*.**
923 **(A)** Sucrose gradient fractionation of stroma from the indicated genotypes. An equal
924 volume of each fraction was analyzed by immunoblots with antibodies against a ribosomal

925 protein from the small (RPS1) and large subunit (RPL33) and mTERF9 (Myc). The
926 Coomassie blue-stained membrane (CBB) of the wild-type (WT) fractions is shown below.
927 **(B)** Polysomal association of mTERF9. Leaf polysomes from complemented *mterf9* plants
928 were fractionated on 15% to 50% sucrose gradients. Fractions were analyzed by
929 immunoblotting with antibodies against mTERF9 (Myc) and ribosomal proteins (RPS1 and
930 RPL2) and RNA electrophoresis on denaturing agarose gel (bottom). The protein and
931 RNA membranes stained with CBB and methylene blue (MB) are shown, respectively.
932 The sedimentation of the free ribosomes (<80S) and polysomes on the gradient was
933 confirmed with a puromycin control.
934
935 **Figure 6. mTERF9 associates with the 16S rRNA in chloroplasts. (A)** mTERF9 RNA
936 ligands were identified by co-immunoprecipitation on stromal extract from the
937 complemented *mterf9* (CP) or wild-type (WT, negative experimental control) with anti-Myc
938 antibodies, followed by RNA hybridization on a chloroplast genome tiling microarray. The
939 efficiency of mTERF9 immunoprecipitation was confirmed by immunoblot analysis with
940 Myc antibodies. Sup: supernatant, IP: immunoprecipitate. **(B)** RIP-chip analysis. The
941 enrichment ratios (ratio of signal in the immunoprecipitation pellet versus supernatant) are
942 plotted according to position on the chloroplast genome after subtracting values obtained
943 in the negative control immunoprecipitation (WT stroma). The RIP-chip assay revealed
944 the predominant enrichment of the 16S rRNA in mTEF9 immunoprecipitate. **(C)**
945 Verification of mTERF9 RNA ligands by qRT-PCR. The levels of immunoprecipitated
946 RNAs were calculated as percent recovery of the total input RNA. **(D)** Slot blotting
947 validation of mTERF9 RNA ligands. RNA purified from the immunoprecipitates and
948 supernatants were applied to slot blots and hybridized with the indicated probes.
949
950 **Figure 7. mTERF9 protein interactome is highly enriched with proteins involved in**
951 **chloroplast ribosome biogenesis. (A)** mTERF9 immunoprecipitation. Untreated or
952 RNase-treated stroma extracts from complemented *mterf9* (CP) or wild-type (WT) plants
953 were used for immunoprecipitation with anti-Myc antibody. The input, flow-through (FT)
954 and immunoprecipitate (IP) fractions were analyzed by immunoblot with anti-Myc
955 antibody. A portion of the Coomassie blue-stained membrane (CBB) showing the

abundance of RbcL as loading control. **(B)** Volcano plots show the enrichment of proteins co-purified with mTERF9 and identified by mass spectrometry in absence or presence of RNase in comparison with control IPs. IPs were performed on biological triplicate. *Y*- and *X*-axis display Log_{10} scale of -Log_{10} adjusted *p*-values (adj_*P*) and Log_2 fold changes (FC) of proteins, respectively. The dashed lines indicate the threshold above which proteins were significantly enriched (*p*-value <0.05 and FC >4). Proteins are color-shaded according to their functional group and the color key provided to the right. ns: not significant. The full lists of mTERF9-associated proteins and their Arabidopsis locus identifiers are available in Supplemental Data Set 1. **(C)** Bar chart showing the number of significant mTERF9 interacting proteins in the functional groups. The same color code than in (B) is used. The "overlap" bar represents common proteins found in mTERF9 protein interactomes in absence of presence of RNase. **(D)** Bar chart depicting the functional analysis of the mTERF9 protein interactomes and showing the 5 terms contained in the top functional annotation cluster identified by DAVID gene analysis online tool using the default parameters (Huang da et al., 2009). GO terms are plotted according to $-Log_{10}$ of their respective adjusted *p*-values. **(E)** Venn diagrams showing the significantly enriched proteins in each functional category in mTERF9 immunoprecipitates. **(F)** Immunoblot validation of mTERF9 interactants identified by co-IP/MS analysis in absence of RNase. Replicate blots were probed with anti-Myc, anti-RH3, anti-RPS1 and anti-RPL33. A replicate of a CBB-stained membrane is shown as input loading control.

Figure 8. mTERF9 directly interacts with some of its *in vivo* protein interactants. (A) Schematic representation of mTERF9 used as bait or prey in the yeast two hybrid assay. **(B)** The yeast two hybrid assay was applied to assess direct interactions of mTERF9 with proteins identified by co-IP/MS analysis and mTERF9 self-association. mTERF9 interacts in yeast with ERA1, a putative 30S ribosomal subunit assembly factor, PSRP2 and RPL1, two plastid ribosomal proteins of the small and large ribosome subunits, CPN60β1 and β3 (CPNB1, B3), two subunits of the CPN60 chaperonin complex and finally itself. The bait vector expressing mTERF9 in fusion with the C-terminal half of the ubiquitin and the transcription factor LexA (Cub-LexA) was co-transformed with prey vectors expressing

the protein candidates fused to the N-terminal half of the ubiquitin and HA tag (Nub-HA) in a yeast reporter strain. Yeast co-transformants were spotted in 10-fold serial dilutions on plates without Trp, Leu (-WL). Positive interactions allow growth on plates without Trp, Leu, His, Ade in presence of 3-aminotriazol (-WLHA + 3-AT). Negative controls were performed using bait or prey empty vectors (EV).

TABLES

Table 1. Chlorophyll *a* fluorescence induction and light-induced PSI absorbance changes. Chlorophyll *a* fluorescence was measured on 2-week-old Arabidopsis plants grown on soil. Representative measurements of chlorophyll *a* fluorescence in the WT, *mterf9* mutants and complemented (CP) lines. Saturating light pulses were given in 20 s intervals during induction (Meurer et al., 1996).

	WT$_h$ (n$_i$=5)	***mterf9* (n=5)**	**CP (n=5)**
Fv/Fm$_a$	0,81 ± 0,00	0,70 ± 0,01	0,81 ± 0,01
Fo	1,00 ± 0,11	1,25 ± 0,05	1,02 ± 0,08
Φ$_{PSIIb}$	0,73 ± 0,01	0,58 ± 0,01	0,72 ± 0,02
NPQ$_c$	0,20 ± 0,02	0,22 ± 0,02	0,20 ± 0,02
Φ$_{PSId}$	0,47 ± 0,02	0,42 ± 0,05	0,41 ± 0.01
Φ$_{PSI\ NDe}$	0,27 ± 0,05	0,48 ± 0,03	0,29 ± 0,04
Φ$_{PSI\ NAf}$	0,28 ± 0,03	0,12 ± 0,05	0,30 ± 0,03
%$_g$ ΔA$_{P700}$	100,00 ± 11,22	67,34 ± 4,65	104,51 ± 14,5

a maximum quantum yield of PSII

b effective quantum yield of PSII (50 µmol photons m^{-2} s^{-1}).

c non-photochemical quenching.

d quantum yield of PSI.

e quantum yield of non-photochemical energy dissipation due to PSI donor side limitation.

f quantum yield of non-photochemical energy dissipation due to PSI acceptor side limitation.

G maximum absorbance of P700 in % of the WT.

[h] the data for the WT were collected along with *mterf9* and an additional Arabidopsis mutant *mda1* (Méteignier et al., 2020). As such, the WT values are the same as in (Méteignier et al., 2020).

[i] number of plants measured.

Figure 1

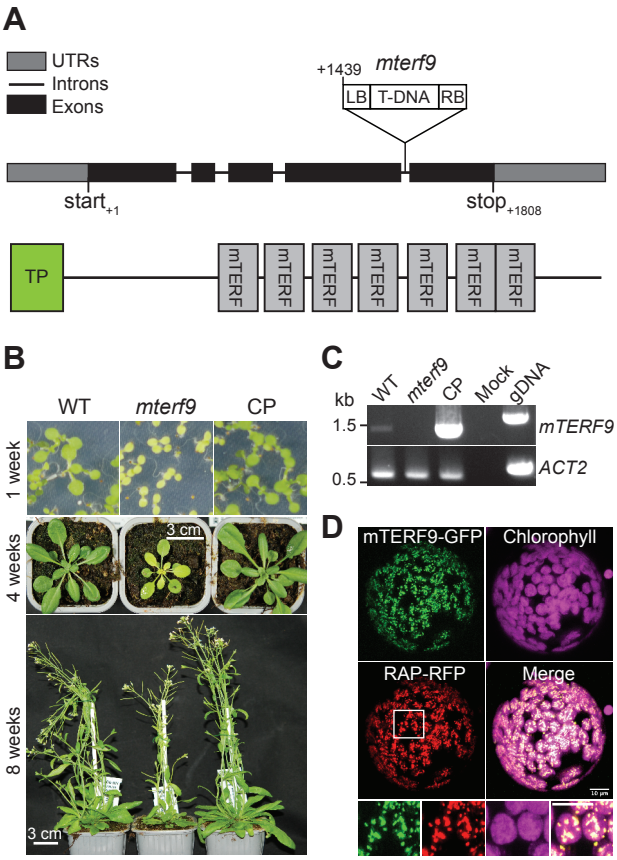

Figure 1. mTERF9 is a chloroplast nucleoid-associated protein required for plant development. (A) Schematic representation of the *mTERF9* gene and protein with the position of the *mterf9* T-DNA insertion. **(B)** Phenotypes of wild-type (WT), *mterf9* and complemented (CP) plants grown in medium or soil at indicated growth stages. **(C)** RT-PCR analysis of *mTERF9* expression in WT, *mterf9* and complemented plants. Genomic DNA (gDNA) was used as positive control for PCR and *ACTIN-2* (*ACT2*) serves as internal control for RT-PCR. **(D)** Subcellular localization of mTERF9-GFP and RAP-GFP fusion proteins in tobacco leaf protoplasts. Close-up views of the framed area are shown below. Scale bar: 5 μm.

Figure 2

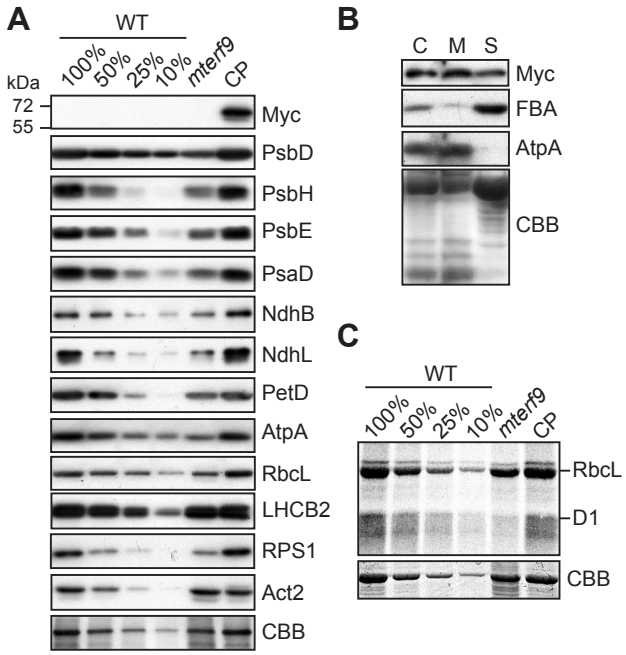

Figure 2. Chloroplast protein accumulation deficiency in *mterf9*. (A) Immunoblot analyses of total leaf protein extracts with antibodies against mTERF9-Myc and subunits of the photosystem I (PsaD), photosystem II (PsbD, PsbH, PsbE,), Cytochrome b_6f (PetD), NADH dehydrogenase (NdhB, NdhL), ATP synthase (AtpA), Rubisco (RbcL), light-harvesting complex II (LHCB2) and ribosome (RPS1) complexes. Replicate membranes were stained with Coomassie Blue (CBB) to show equal protein loading. **(B)** mTERF9 localizes to the stroma and chloroplast membranes. Isolated chloroplasts were lysed in hypotonic buffer and membrane and soluble protein fractions were separated by centrifugation. Chloroplast (C), soluble (S), and membrane (M) protein fractions were analyzed by immunoblotting using antibodies against Myc epitope, a stromal protein (Fructose-bisphosphate aldolase 1) and a membrane associated subunit of the ATP synthase complex (AtpA). The Coomassie Blue (CBB) stained membrane is shown. **(C)** *In vivo* chloroplast translation assays. Leaf discs from the indicated genotypes were pulsed-labelled with ^{35}S-Methionine and neosynthesized proteins were separated by SDS-PAGE and visualized by autoradiography. The CBB stained gel is shown below and serves as equal loading control.

Figure 3

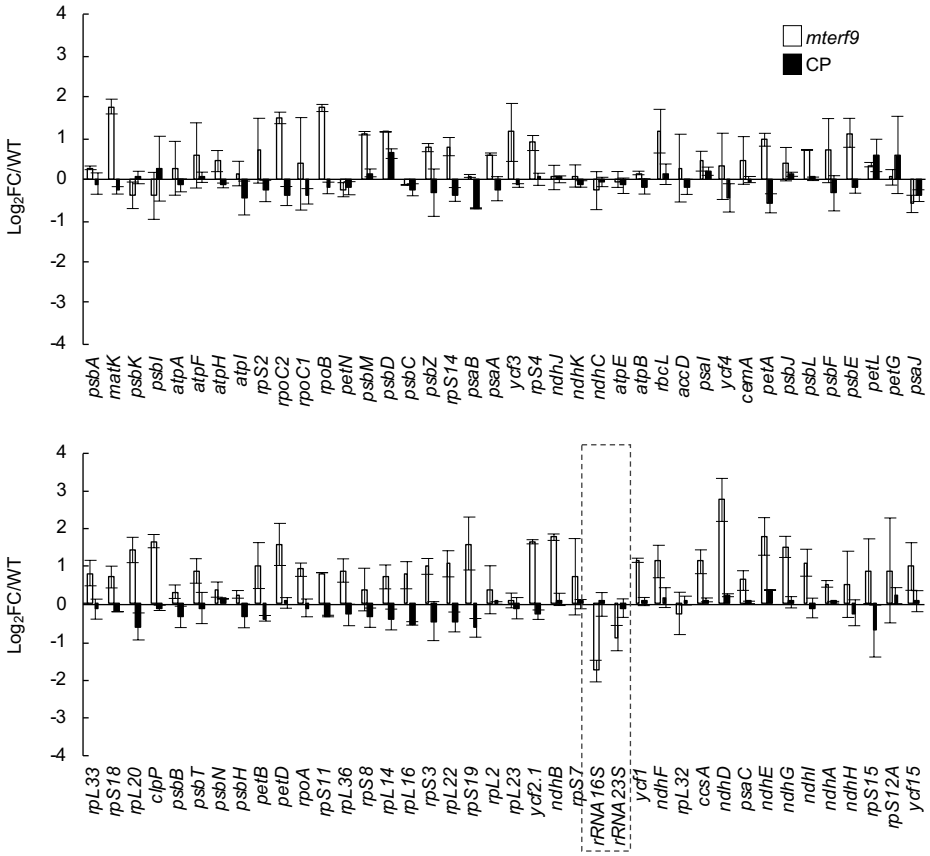

Figure 3. Steady state levels of chloroplast gene transcripts in Arabidopsis in *mterf9* and CP plants. Transcript levels were determined by qRT-PCR and are displayed as the $\log_2$ fold change (FC) between values obtained for the mutant or the complemented plants and the WT plants. Genes are ordered according to their genome positions. The nuclear *ACT2* and *TIP41* genes were used for data normalization. The values from two biological replicates performed each with technical triplicate were averaged per genotype and standard errors are indicated.

Figure 4

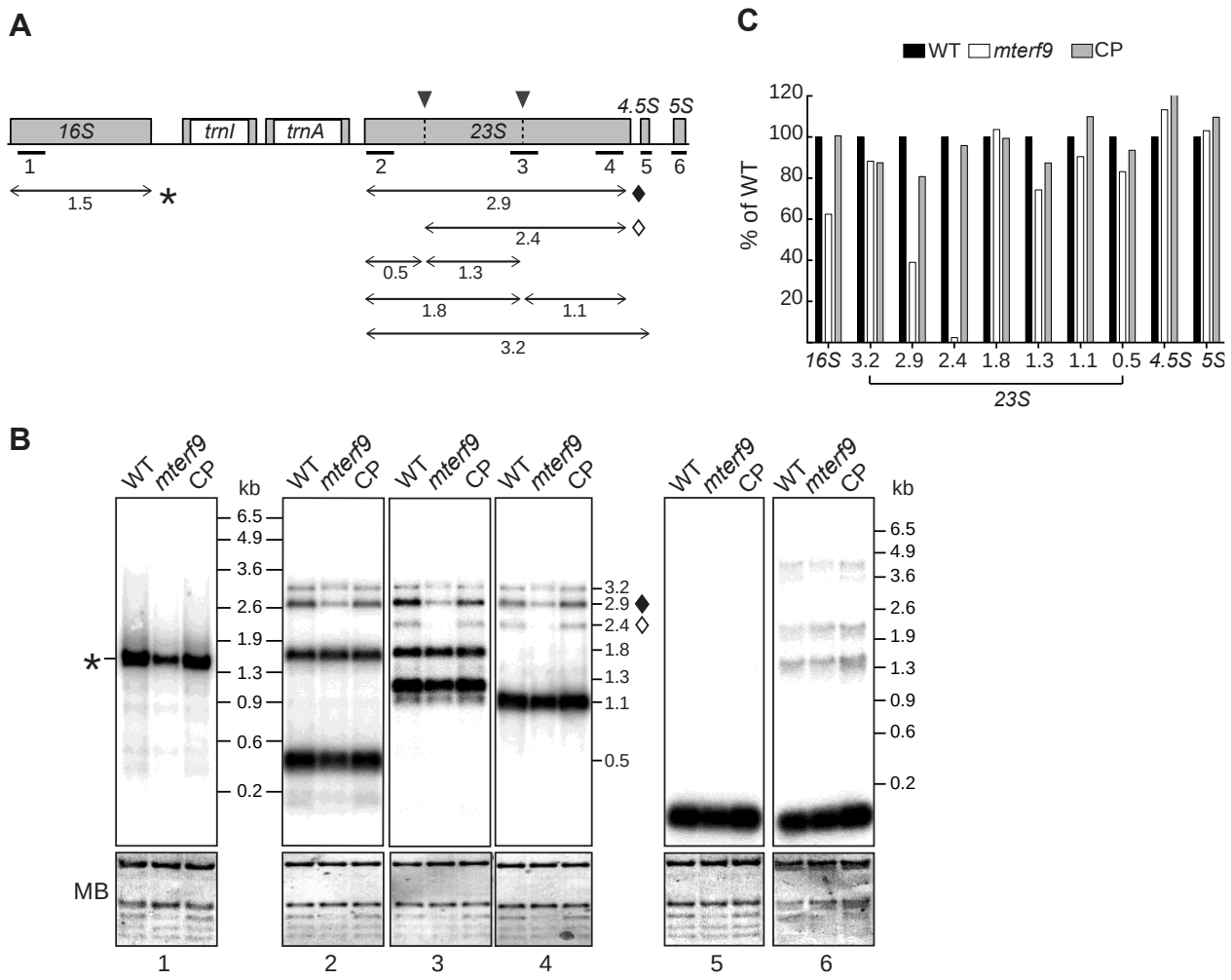

Figure 4. Defects in the 16S and 23S rRNA accumulation in *mterf9* plants. (A) Schematic representation of the chloroplast rRNA operon. Exons and introns are represented by gray and white boxes, respectively. The positions of the probes used for RNA blot hybridization are indicated beneath the map. The *23S* rRNA hidden breaks positions are shown above the gene with black arrowheads. The major accumulating transcripts for the 16S and 23S rRNA genes are mapped with arrows and their size is given in kb below. Transcripts specifically impaired in the *mterf9* are indicated with symbols. **(B)** Total leaf RNA (0.5 μg) was analyzed by RNA gel blot hybridization using probes diagrammed in (A). **(C)** Relative quantification to wild-type (WT) in the accumulation of the chloroplast rRNAs in *mterf9* and complemented (CP) plants.

Figure 5

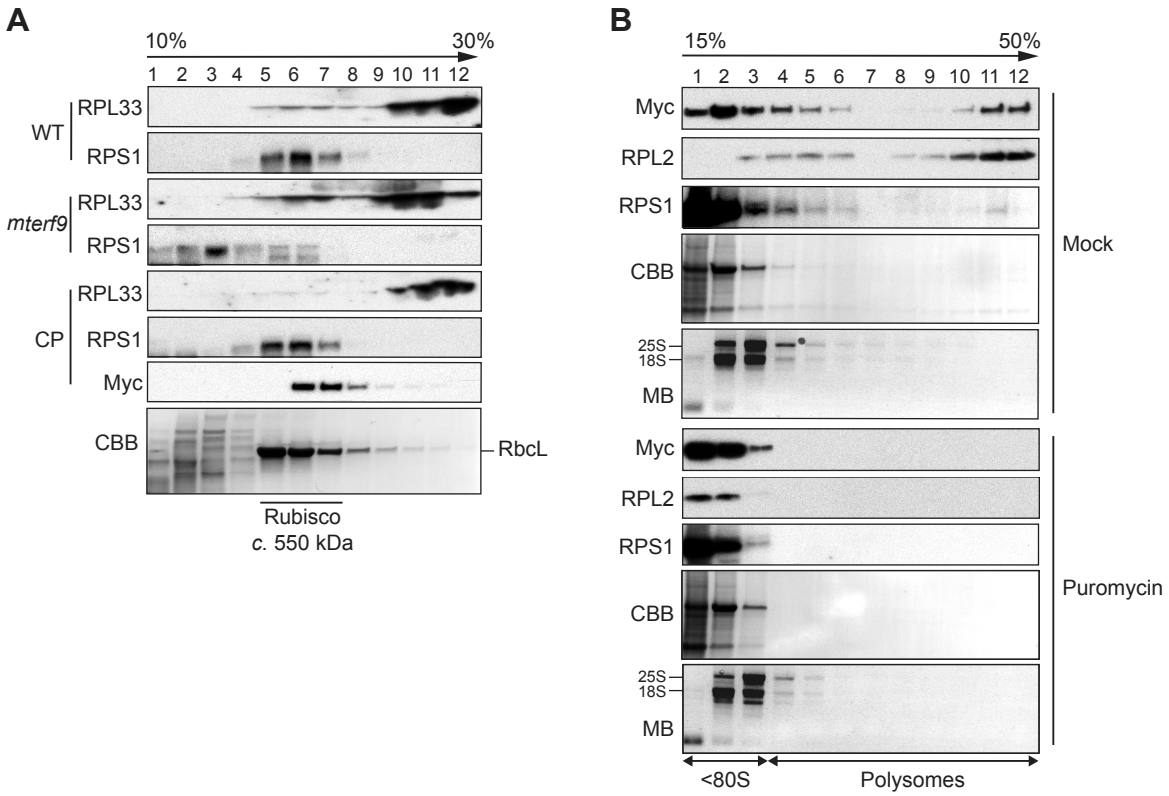

Figure 5. mTERF9 associates with chloroplast ribosomes and polysomes *in vivo*. **(A)** Sucrose gradient fractionation of stroma from the indicated genotypes. An equal volume of each fraction was analyzed by immunoblots with antibodies against a ribosomal protein from the small (RPS1) and large subunit (RPL33) and mTERF9 (Myc). The Coomassie blue-stained membrane (CBB) of the wild-type (WT) fractions is shown below. **(B)** Polysomal association of mTERF9. Leaf polysomes from complemented *mterf9* plants were fractionated on 15% to 50% sucrose gradients. Fractions were analyzed by immunoblotting with antibodies against mTERF9 (Myc) and ribosomal proteins (RPS1 and RPL2) and RNA electrophoresis on denaturing agarose gel (bottom). The protein and RNA membranes stained with CBB and methylene blue (MB) are shown, respectively. The sedimentation of the free ribosomes (<80S) and polysomes on the gradient was confirmed with a puromycin control.

Figure 6

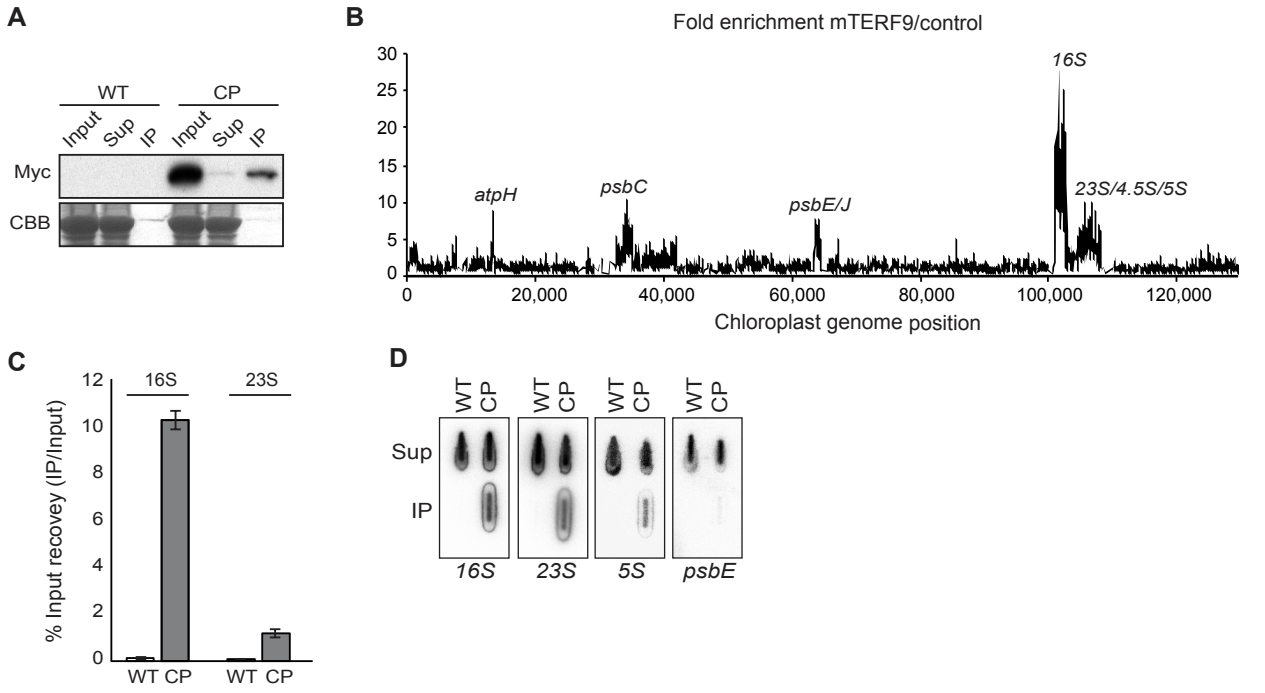

Figure 6. mTERF9 associates with the 16S rRNA in chloroplasts. (A) mTERF9 RNA ligands were identified by co-immunoprecipitation on stromal extract from the complemented *mterf9* (CP) or wild-type (WT, negative experimental control) with anti-Myc antibodies, followed by RNA hybridization on a chloroplast genome tiling microarray. The efficiency of mTERF9 immunoprecipitation was confirmed by immunoblot analysis with Myc antibodies. Sup: supernatant, IP: immunoprecipitate. **(B)** RIP-chip analysis. The enrichment ratios (ratio of signal in the immunoprecipitation pellet versus supernatant) are plotted according to position on the chloroplast genome after subtracting values obtained in the negative control immunoprecipitation (WT stroma). The RIP-chip assay revealed the predominant enrichment of the 16S rRNA in mTEF9 immunoprecipitate. **(C)** Verification of mTERF9 RNA ligands by qRT-PCR. The levels of immunoprecipitated RNAs were calculated as percent recovery of the total input RNA. **(D)** Slot blotting validation of mTERF9 RNA ligands. RNA purified from the immunoprecipitates and supernatants were applied to slot blots and hybridized with the indicated probes.

Figure 7

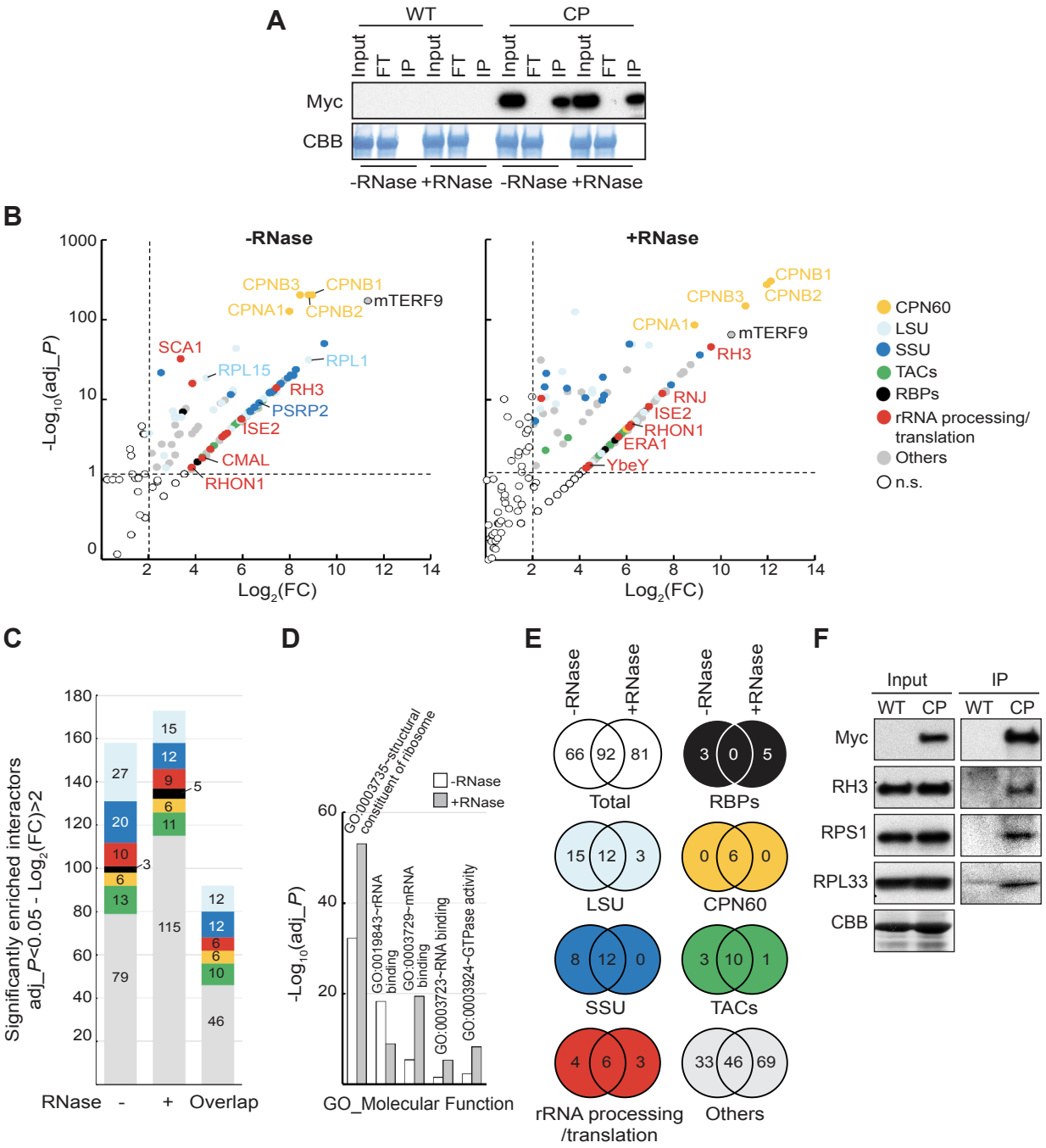

Figure 7. mTERF9 protein interactome is highly enriched with proteins involved in chloroplast ribosome biogenesis. (A) mTERF9 immunoprecipitation. Untreated or RNase-treated stroma extracts from complemented *mterf9* (CP) or wild-type (WT) plants were used for immunoprecipitation with anti-Myc antibody. The input, flow-through (FT) and immunoprecipitate (IP) fractions were analyzed by immunoblot with anti-Myc antibody. A portion of the Coomassie blue-stained membrane (CBB) showing the abundance of RbcL as loading control. **(B)** Volcano plots show the enrichment of proteins co-purified with mTERF9 and identified by mass spectrometry in absence or presence of RNase in comparison with control IPs. IPs were performed on biological triplicate. *Y*- and *X*-axis display Log_{10} scale of -Log_{10} adjusted *p*-values (adj_*P*) and Log_2 fold changes (FC) of proteins, respectively. The dashed lines indicate the threshold above which proteins were significantly enriched (*p*-value <0.05 and FC >4). Proteins are color-shaded according to their functional group and the color key provided to the right. ns: not significant. The full lists of mTERF9-associated proteins and their Arabidopsis locus identifiers are available in Supplemental Data Set 1. **(C)** Bar chart showing the number of significant mTERF9 interacting proteins in the functional groups. The same color code than in (B) is used. The “overlap” bar represents common proteins found in mTERF9 protein interactomes in absence of presence of RNase. **(D)** Bar chart depicting the functional analysis of the mTERF9 protein interactomes and showing the 5 terms contained in the top functional annotation cluster identified by DAVID gene analysis online tool using the default parameters (Huang da et al., 2009). GO terms are plotted according to $-Log_{10}$ of their respective adjusted *p*-values. **(E)** Venn diagrams showing the significantly enriched proteins in each functional category in mTERF9 immunoprecipitates. **(F)** Immunoblot validation of mTERF9 interactants identified by co-IP/MS analysis in absence of RNase. Replicate blots were probed with anti-Myc, anti-RH3, anti-RPS1 and anti-RPL33. A replicate of a CBB-stained membrane is shown as input loading control.

Figure 8

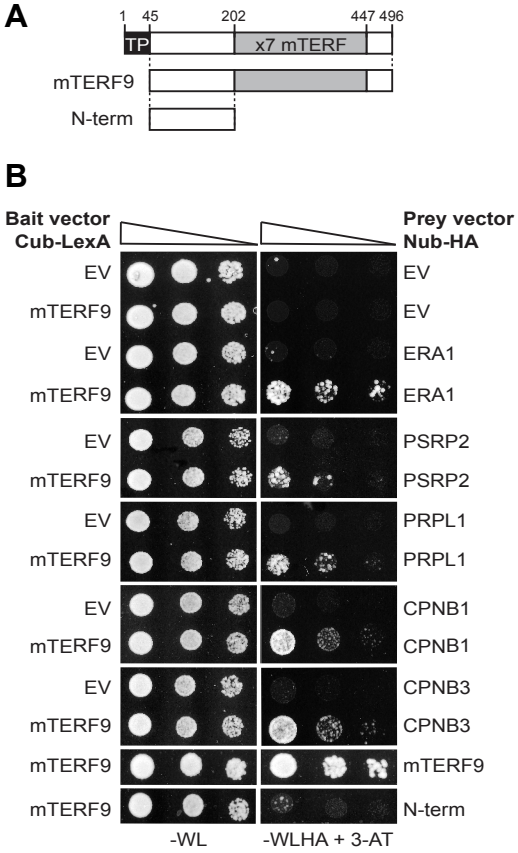

Figure 8. mTERF9 directly interacts with some of its *in vivo* protein interactants. (A) Schematic representation of mTERF9 used as bait or prey in the yeast two hybrid assay. **(B)** The yeast two hybrid assay was applied to assess direct interactions of mTERF9 with proteins identified by co-IP/MS analysis and mTERF9 self-association. mTERF9 interacts in yeast with ERA1, a putative 30S ribosomal subunit assembly factor, PSRP2 and RPL1, two plastid ribosomal proteins of the small and large ribosome subunits, CPN60β1 and β3 (CPNB1, B3), two subunits of the CPN60 chaperonin complex and finally itself. The bait vector expressing mTERF9 in fusion with the C-terminal half of the ubiquitin and the transcription factor LexA (Cub-LexA) was co-transformed with prey vectors expressing the protein candidates fused to the N-terminal half of the ubiquitin and HA tag (Nub-HA) in a yeast reporter strain. Yeast co-transformants were spotted in 10-fold serial dilutions on plates without Trp, Leu (-WL). Positive interactions allow growth on plates without Trp, Leu, His, Ade in presence of 3-aminotriazol (-WLHA + 3-AT). Negative controls were performed using bait or prey empty vectors (EV).

Parsed Citations

Adam, Z., Aviv-Sharon, E., Keren-Paz, A., Naveh, L., Rozenberg, M., Savidor, A., and Chen, J. (2019). The Chloroplast Envelope Protease FTSH11 - Interaction With CPN60 and Identification of Potential Substrates. Front Plant Sci 10, 428.
Pubmed: Author and Title
Google Scholar: Author Only Title Only Author and Title

Anders, S., and Huber, W. (2010). Differential expression analysis for sequence count data. Genome Biol 11, R106.
Pubmed: Author and Title
Google Scholar: Author Only Title Only Author and Title

Asakura, Y., Galarneau, E., Watkins, K.P., Barkan, A., and van Wijk, K.J. (2012). Chloroplast RH3 DEAD box RNA helicases in maize and Arabidopsis function in splicing of specific group II introns and affect chloroplast ribosome biogenesis. Plant Physiol 159, 961-974.
Pubmed: Author and Title
Google Scholar: Author Only Title Only Author and Title

Babiychuk, E., Vandepoele, K., Wissing, J., Garcia-Diaz, M., De Rycke, R., Akbari, H., Joubes, J., Beeckman, T., Jansch, L., Frentzen, M., Van Montagu, M.C., and Kushnir, S. (2011). Plastid gene expression and plant development require a plastidic protein of the mitochondrial transcription termination factor family. Proc Natl Acad Sci U S A 108, 6674-6679.
Pubmed: Author and Title
Google Scholar: Author Only Title Only Author and Title

Barkan, A. (1993). Nuclear Mutants of Maize with Defects in Chloroplast Polysome Assembly Have Altered Chloroplast RNA Metabolism. Plant Cell 5, 389-402.
Pubmed: Author and Title
Google Scholar: Author Only Title Only Author and Title

Barkan, A. (1998). Approaches to investigating nuclear genes that function in chloroplast biogenesis in land plants. Method Enzymol 297, 38-57.
Pubmed: Author and Title
Google Scholar: Author Only Title Only Author and Title

Barraclough, R., and Ellis, R.J. (1980). Protein synthesis in chloroplasts. IX. Assembly of newly-synthesized large subunits into ribulose bisphosphate carboxylase in isolated intact pea chloroplasts. Biochim Biophys Acta 608, 19-31.
Pubmed: Author and Title
Google Scholar: Author Only Title Only Author and Title

Belcher, S., Williams-Carrier, R., Stiffler, N., and Barkan, A. (2015). Large-scale genetic analysis of chloroplast biogenesis in maize. Biochim Biophys Acta 1847, 1004-1016.
Pubmed: Author and Title
Google Scholar: Author Only Title Only Author and Title

Berglund, A.K., Pujol, C., Duchene, A.M., and Glaser, E. (2009). Defining the determinants for dual targeting of amino acyl-tRNA synthetases to mitochondria and chloroplasts. J Mol Biol 393, 803-814.
Pubmed: Author and Title
Google Scholar: Author Only Title Only Author and Title

Bobik, K., McCray, T.N., Ernest, B., Fernandez, J.C., Howell, K.A., Lane, T., Staton, M., and Burch-Smith, T.M. (2017). The chloroplast RNA helicase ISE2 is required for multiple chloroplast RNA processing steps in Arabidopsis thaliana. Plant J 91, 114-131.
Pubmed: Author and Title
Google Scholar: Author Only Title Only Author and Title

Bryant, N., Lloyd, J., Sweeney, C., Myouga, F., and Meinke, D. (2011). Identification of nuclear genes encoding chloroplast-localized proteins required for embryo development in Arabidopsis. Plant Physiol 155, 1678-1689.
Pubmed: Author and Title
Google Scholar: Author Only Title Only Author and Title

Chicher, J., Simonetti, A., Kuhn, L., Schaeffer, L., Hammann, P., Eriani, G., and Martin, F. (2015). Purification of mRNA-programmed translation initiation complexes suitable for mass spectrometry analysis. Proteomics 15, 2417-2425.
Pubmed: Author and Title
Google Scholar: Author Only Title Only Author and Title

Ding, S., Zhang, Y., Hu, Z., Huang, X., Zhang, B., Lu, Q., Wen, X., Wang, Y., and Lu, C. (2019). mTERF5 Acts as a Transcriptional Pausing Factor to Positively Regulate Transcription of Chloroplast psbEFLJ. Mol Plant 12, 1259-1277.
Pubmed: Author and Title
Google Scholar: Author Only Title Only Author and Title

Olinares, P.D., Ponnala, L., and van Wijk, K.J. (2010). Megadalton complexes in the chloroplast stroma of Arabidopsis thaliana characterized by size exclusion chromatography, mass spectrometry, and hierarchical clustering. Mol Cell Proteomics 9, 1594-1615.
Pubmed: Author and Title
Google Scholar: Author Only Title Only Author and Title

Gietz, R.D., and Schiestl, R.H. (2007). High-efficiency yeast transformation using the LiAc/SS carrier DNA/PEG method. Nature Protocols 2, 31-34.

Pubmed: Author and Title
Google Scholar: Author Only Title Only Author and Title

Graf, M., Arenz, S., Huter, P., Donhofer, A., Novacek, J., and Wilson, D.N. (2017). Cryo-EM structure of the spinach chloroplast ribosome reveals the location of plastid-specific ribosomal proteins and extensions. Nucleic Acids Res 45, 2887-2896.
Pubmed: Author and Title
Google Scholar: Author Only Title Only Author and Title

Grove, T.Z., Cortajarena, A.L., and Regan, L. (2008). Ligand binding by repeat proteins: natural and designed. Curr Opin Struct Biol 18, 507-515.
Pubmed: Author and Title
Google Scholar: Author Only Title Only Author and Title

Gu, L., Xu, T., Lee, K., Lee, K.H., and Kang, H. (2014). A chloroplast-localized DEAD-box RNA helicase AtRH3 is essential for intron splicing and plays an important role in the growth and stress response in Arabidopsis thaliana. Plant Physiol Biochem 82, 309-318.
Pubmed: Author and Title
Google Scholar: Author Only Title Only Author and Title

Hammani, K., and Barkan, A. (2014). An mTERF domain protein functions in group II intron splicing in maize chloroplasts. Nucleic Acids Res 42, 5033-5042.
Pubmed: Author and Title
Google Scholar: Author Only Title Only Author and Title

Hammani, K., Bonnard, G., Bouchoucha, A., Gobert, A., Pinker, F., Salinas, T., and Giege, P. (2014). Helical repeats modular proteins are major players for organelle gene expression. Biochimie 100C, 141-150.
Pubmed: Author and Title
Google Scholar: Author Only Title Only Author and Title

Hotto, A.M., Castandet, B., Gilet, L., Higdon, A., Condon, C., and Stern, D.B. (2015). Arabidopsis chloroplast mini-ribonuclease III participates in rRNA maturation and intron recycling. Plant Cell 27, 724-740.
Pubmed: Author and Title
Google Scholar: Author Only Title Only Author and Title

Hristou, A., Gerlach, I., Stolle, D.S., Neumann, J., Bischoff, A., Dunschede, B., Nowaczyk, M.M., Zoschke, R., and Schunemann, D. (2019). Ribosome-Associated Chloroplast SRP54 Enables Efficient Cotranslational Membrane Insertion of Key Photosynthetic Proteins. Plant Cell 31, 2734-2750.
Pubmed: Author and Title
Google Scholar: Author Only Title Only Author and Title

Hsu, Y.W., Wang, H.J., Hsieh, M.H., Hsieh, H.L., and Jauh, G.Y. (2014). Arabidopsis mTERF15 is required for mitochondrial nad2 intron 3 splicing and functional complex I activity. PLoS One 9, e112360.
Pubmed: Author and Title
Google Scholar: Author Only Title Only Author and Title

Huang da, W., Sherman, B.T., and Lempicki, R.A. (2009). Systematic and integrative analysis of large gene lists using DAVID bioinformatics resources. Nat Protoc 4, 44-57.
Pubmed: Author and Title
Google Scholar: Author Only Title Only Author and Title

Jimenez-Menendez, N., Fernandez-Millan, P., Rubio-Cosials, A., Arnan, C., Montoya, J., Jacobs, H.T., Bernado, P., Coll, M., Uson, I., and Sola, M. (2010). Human mitochondrial mTERF wraps around DNA through a left-handed superhelical tandem repeat. Nat Struct Mol Biol 17, 891-893.
Pubmed: Author and Title
Google Scholar: Author Only Title Only Author and Title

Kleine, T. (2012). Arabidopsis thaliana mTERF proteins: evolution and functional classification. Front Plant Sci 3, 233.
Pubmed: Author and Title
Google Scholar: Author Only Title Only Author and Title

Kleine, T., and Leister, D. (2015). Emerging functions of mammalian and plant mTERFs. Biochim Biophys Acta 1847, 786-797.
Pubmed: Author and Title
Google Scholar: Author Only Title Only Author and Title

Kleinknecht, L., Wang, F., Stube, R., Philippar, K., Nickelsen, J., and Bohne, A.V. (2014). RAP, the sole octotricopeptide repeat protein in Arabidopsis, is required for chloroplast 16S rRNA maturation. Plant Cell 26, 777-787.
Pubmed: Author and Title
Google Scholar: Author Only Title Only Author and Title

Klughammer, C., and Schreiber, U. (1994). An improved method, using saturating light pulses, for the determination of photosystem I quantum yield via P700+-absorbance changes at 830 nm. Planta 192, 261-268.
Pubmed: Author and Title
Google Scholar: Author Only Title Only Author and Title

Kunst, L. (1998). Preparation of physiologically active chloroplasts from Arabidopsis. Methods Mol Biol 82, 43-48.
Pubmed: Author and Title

Google Scholar: Author Only Title Only Author and Title

Lamesch, P., Berardini, T.Z., Li, D., Swarbreck, D., Wilks, C., Sasidharan, R., Muller, R., Dreher, K., Alexander, D.L., Garcia-Hernandez, M., Karthikeyan, A.S., Lee, C.H., Nelson, W.D., Ploetz, L., Singh, S., Wensel, A., and Huala, E. (2012). The Arabidopsis Information Resource (TAIR): improved gene annotation and new tools. Nucleic Acids Res 40, D1202-1210.

Pubmed: Author and Title
Google Scholar: Author Only Title Only Author and Title

Lee, K.H., Park, J., Williams, D.S., Xiong, Y., Hwang, I., and Kang, B.H. (2013). Defective chloroplast development inhibits maintenance of normal levels of abscisic acid in a mutant of the Arabidopsis RH3 DEAD-box protein during early post-germination growth. Plant J 73, 720-732.

Pubmed: Author and Title
Google Scholar: Author Only Title Only Author and Title

Linder, T., Park, C.B., Asin-Cayuela, J., Pellegrini, M., Larsson, N.G., Falkenberg, M., Samuelsson, T., and Gustafsson, C.M. (2005). A family of putative transcription termination factors shared amongst metazoans and plants. Curr Genet 48, 265-269.

Pubmed: Author and Title
Google Scholar: Author Only Title Only Author and Title

Liu, J., Zhou, W., Liu, G., Yang, C., Sun, Y., Wu, W., Cao, S., Wang, C., Hai, G., Wang, Z., Bock, R., Huang, J., and Cheng, Y. (2015). The conserved endoribonuclease YbeY is required for chloroplast ribosomal RNA processing in Arabidopsis. Plant Physiol 168, 205-221.

Pubmed: Author and Title
Google Scholar: Author Only Title Only Author and Title

Liu, S., Zheng, L., Jia, J., Guo, J., Zheng, M., Zhao, J., Shao, J., Liu, X., An, L., Yu, F., and Qi, Y. (2019). Chloroplast Translation Elongation Factor EF-Tu/SVR11 Is Involved in var2-Mediated Leaf Variegation and Leaf Development in Arabidopsis. Front Plant Sci 10, 295.

Pubmed: Author and Title
Google Scholar: Author Only Title Only Author and Title

Loh, P.C., Morimoto, T., Matsuo, Y., Oshima, T., and Ogasawara, N. (2007). The GTP-binding protein YqeH participates in biogenesis of the 30S ribosome subunit in Bacillus subtilis. Genes Genet Syst 82, 281-289.

Pubmed: Author and Title
Google Scholar: Author Only Title Only Author and Title

Majeran, W., Friso, G., Asakura, Y., Qu, X., Huang, M., Ponnala, L., Watkins, K.P., Barkan, A., and van Wijk, K.J. (2012). Nucleoid-enriched proteomes in developing plastids and chloroplasts from maize leaves: a new conceptual framework for nucleoid functions. Plant Physiol 158, 156-189.

Pubmed: Author and Title
Google Scholar: Author Only Title Only Author and Title

Méteignier, L.V., Ghandour, R., Meierhoff, K., Zimmerman, A., Chicher, J., Baumberger, N., Alioua, A., Meurer, J., Zoschke, R., and Hammani, K. (2020). The Arabidopsis mTERF-repeat MDA1 protein plays a dual function in transcription and stabilization of specific chloroplast transcripts within the psbE and ndhH operons. New Phytologist DOI: 10.1111/nph.16625.

Pubmed: Author and Title
Google Scholar: Author Only Title Only Author and Title

Meurer, J., Meierhoff, K., and Westhoff, P. (1996). Isolation of high-chlorophyll-fluorescence mutants of Arabidopsis thaliana and their characterisation by spectroscopy, immunoblotting and northern hybridisation. Planta 198, 385-396.

Pubmed: Author and Title
Google Scholar: Author Only Title Only Author and Title

Miura, E., Kato, Y., Matsushima, R., Albrecht, V., Laalami, S., and Sakamoto, W. (2007). The balance between protein synthesis and degradation in chloroplasts determines leaf variegation in Arabidopsis yellow variegated mutants. Plant Cell 19, 1313-1328.

Pubmed: Author and Title
Google Scholar: Author Only Title Only Author and Title

Möckli, N., Deplazes, A., and Auerbach, D. (2008). Finding new protein interactions using the DUALhunter system. Nature Methods 5, i-ii.

Pubmed: Author and Title
Google Scholar: Author Only Title Only Author and Title

Mokry, M., Nijman, I.J., van Dijken, A., Benjamins, R., Heidstra, R., Scheres, B., and Cuppen, E. (2011). Identification of factors required for meristem function in Arabidopsis using a novel next generation sequencing fast forward genetics approach. BMC Genomics 12, 256.

Pubmed: Author and Title
Google Scholar: Author Only Title Only Author and Title

Nishimura, K., Ashida, H., Ogawa, T., and Yokota, A. (2010). A DEAD box protein is required for formation of a hidden break in Arabidopsis chloroplast 23S rRNA. Plant J 63, 766-777.

Pubmed: Author and Title
Google Scholar: Author Only Title Only Author and Title

Nunez-Delegido, E., Robles, P., Ferrandez-Ayela, A., and Quesada, V. (2019). Functional analysis of mTERF5 and mTERF9 contribution

to salt tolerance, plastid gene expression and retrograde signalling in Arabidopsis thaliana. Plant Biol (Stuttg) DOI: 10.1111/plb.13084
Pubmed: Author and Title
Google Scholar: Author Only Title Only Author and Title

Ostheimer, G.J., Williams-Carrier, R., Belcher, S., Osborne, E., Gierke, J., and Barkan, A. (2003). Group II intron splicing factors derived by diversification of an ancient RNA-binding domain. EMBO J 22, 3919-3929.
Pubmed: Author and Title
Google Scholar: Author Only Title Only Author and Title

Peng, L., Fukao, Y., Myouga, F., Motohashi, R., Shinozaki, K., and Shikanai, T. (2011). A chaperonin subunit with unique structures is essential for folding of a specific substrate. PLoS Biol 9, e1001040.
Pubmed: Author and Title
Google Scholar: Author Only Title Only Author and Title

Perez-Riverol, Y., Csordas, A., Bai, J., Bernal-Llinares, M., Hewapathirana, S., Kundu, D.J., Inuganti, A., Griss, J., Mayer, G., Eisenacher, M., Perez, E., Uszkoreit, J., Pfeuffer, J., Sachsenberg, T., Yilmaz, S., Tiwary, S., Cox, J., Audain, E., Walzer, M., Jarnuczak, A.F., Ternent, T., Brazma, A., and Vizcaino, J.A. (2019). The PRIDE database and related tools and resources in 2019: improving support for quantification data. Nucleic Acids Res 47, D442-D450.
Pubmed: Author and Title
Google Scholar: Author Only Title Only Author and Title

Robles, P., Micol, J.L., and Quesada, V. (2015). Mutations in the plant-conserved MTERF9 alter chloroplast gene expression, development and tolerance to abiotic stress in Arabidopsis thaliana. Physiol Plant 154, 297-313.
Pubmed: Author and Title
Google Scholar: Author Only Title Only Author and Title

Robles, P., Navarro-Cartagena, S., Ferrandez-Ayela, A., Nunez-Delegido, E., and Quesada, V. (2018). The Characterization of Arabidopsis mterf6 Mutants Reveals a New Role for mTERF6 in Tolerance to Abiotic Stress. Int J Mol Sci 19.
Pubmed: Author and Title
Google Scholar: Author Only Title Only Author and Title

Romani, I., Manavski, N., Morosetti, A., Tadini, L., Maier, S., Kuhn, K., Ruwe, H., Schmitz-Linneweber, C., Wanner, G., Leister, D., and Kleine, T. (2015). A Member of the Arabidopsis Mitochondrial Transcription Termination Factor Family Is Required for Maturation of Chloroplast Transfer RNAIle(GAU). Plant Physiol 169, 627-646.
Pubmed: Author and Title
Google Scholar: Author Only Title Only Author and Title

Rubinson, E.H., and Eichman, B.F. (2012). Nucleic acid recognition by tandem helical repeats. Curr Opin Struct Biol 22, 101-109.
Pubmed: Author and Title
Google Scholar: Author Only Title Only Author and Title

Sayed, A., Matsuyama, S., and Inouye, M. (1999). Era, an essential Escherichia coli small G-protein, binds to the 30S ribosomal subunit. Biochem Biophys Res Commun 264, 51-54.
Pubmed: Author and Title
Google Scholar: Author Only Title Only Author and Title

Shajani, Z., Sykes, M.T., and Williamson, J.R. (2011). Assembly of bacterial ribosomes. Annu Rev Biochem 80, 501-526.
Pubmed: Author and Title
Google Scholar: Author Only Title Only Author and Title

Sharwood, R.E., Halpert, M., Luro, S., Schuster, G., and Stern, D.B. (2011). Chloroplast RNase J compensates for inefficient transcription termination by removal of antisense RNA. RNA 17, 2165-2176.
Pubmed: Author and Title
Google Scholar: Author Only Title Only Author and Title

Singh, B.N., Mishra, R.N., Agarwal, P.K., Goswami, M., Nair, S., Sopory, S.K., and Reddy, M.K. (2004). A pea chloroplast translation elongation factor that is regulated by abiotic factors. Biochem Biophys Res Commun 320, 523-530.
Pubmed: Author and Title
Google Scholar: Author Only Title Only Author and Title

Spahr, H., Samuelsson, T., Hallberg, B.M., and Gustafsson, C.M. (2010). Structure of mitochondrial transcription termination factor 3 reveals a novel nucleic acid-binding domain. Biochem Biophys Res Commun 397, 386-390.
Pubmed: Author and Title
Google Scholar: Author Only Title Only Author and Title

Stoppel, R., and Meurer, J. (2012). The cutting crew - ribonucleases are key players in the control of plastid gene expression. J Exp Bot 63, 1663-1673.
Pubmed: Author and Title
Google Scholar: Author Only Title Only Author and Title

Stoppel, R., Manavski, N., Schein, A., Schuster, G., Teubner, M., Schmitz-Linneweber, C., and Meurer, J. (2012). RHON1 is a novel ribonucleic acid-binding protein that supports RNase E function in the Arabidopsis chloroplast. Nucleic Acids Res 40, 8593-8606.
Pubmed: Author and Title
Google Scholar: Author Only Title Only Author and Title

Suo, J., Zhao, Q., David, L., Chen, S., and Dai, S. (2017). Salinity Response in Chloroplasts: Insights from Gene Characterization. Int J Mol Sci 18, 1011.
Pubmed: Author and Title
Google Scholar: Author Only Title Only Author and Title

Suwastika, I.N., Denawa, M., Yomogihara, S., Im, C.H., Bang, W.Y., Ohniwa, R.L., Bahk, J.D., Takeyasu, K., and Shiina, T. (2014). Evidence for lateral gene transfer (LGT) in the evolution of eubacteria-derived small GTPases in plant organelles. Front Plant Sci 5, 678.
Pubmed: Author and Title
Google Scholar: Author Only Title Only Author and Title

Tiller, N., and Bock, R. (2014). The translational apparatus of plastids and its role in plant development. Mol Plant 7, 1105-1120.
Pubmed: Author and Title
Google Scholar: Author Only Title Only Author and Title

Trosch, R., Barahimipour, R., Gao, Y., Badillo-Corona, J.A., Gotsmann, V.L., Zimmer, D., Muhlhaus, T., Zoschke, R., and Willmund, F. (2018). Commonalities and differences of chloroplast translation in a green alga and land plants. Nat Plants 4, 564-575.
Pubmed: Author and Title
Google Scholar: Author Only Title Only Author and Title

Tsugeki, R., and Nishimura, M. (1993). Interaction of homologues of Hsp70 and Cpn60 with ferredoxin-NADP+ reductase upon its import into chloroplasts. FEBS Lett 320, 198-202.
Pubmed: Author and Title
Google Scholar: Author Only Title Only Author and Title

Tzafrir, I., Pena-Muralla, R., Dickerman, A., Berg, M., Rogers, R., Hutchens, S., Sweeney, T.C., McElver, J., Aux, G., Patton, D., and Meinke, D. (2004). Identification of genes required for embryo development in Arabidopsis. Plant Physiol 135, 1206-1220.
Pubmed: Author and Title
Google Scholar: Author Only Title Only Author and Title

Xiong, H.B., Wang, J., Huang, C., Rochaix, J.D., Lin, F.M., Zhang, J.X., Ye, L.S., Shi, X.H., Yu, Q.B., and Yang, Z.N. (2020). mTERF8, a Member of the Mitochondrial Transcription Termination Factor Family, Is Involved in the Transcription Termination of Chloroplast Gene psbJ. Plant Physiol 182, 408-423.
Pubmed: Author and Title
Google Scholar: Author Only Title Only Author and Title

Xu, D., Leister, D., and Kleine, T. (2017). Arabidopsis thaliana mTERF10 and mTERF11, but Not mTERF12, Are Involved in the Response to Salt Stress. Front Plant Sci 8, 1213.
Pubmed: Author and Title
Google Scholar: Author Only Title Only Author and Title

Yakubovskaya, E., Mejia, E., Byrnes, J., Hambardjieva, E., and Garcia-Diaz, M. (2010). Helix unwinding and base flipping enable human MTERF1 to terminate mitochondrial transcription. Cell 141, 982-993.
Pubmed: Author and Title
Google Scholar: Author Only Title Only Author and Title

Yamamoto, T., Burke, J., Autz, G., and Jagendorf, A.T. (1981). Bound Ribosomes of Pea Chloroplast Thylakoid Membranes: Location and Release in Vitro by High Salt, Puromycin, and RNase. Plant Physiol 67, 940-949.
Pubmed: Author and Title
Google Scholar: Author Only Title Only Author and Title

Zhang, S., Zhou, H., Yu, F., Bai, C., Zhao, Q., He, J., and Liu, C. (2016). Structural insight into the cooperation of chloroplast chaperonin subunits. BMC Biol 14, 29.
Pubmed: Author and Title
Google Scholar: Author Only Title Only Author and Title

Zhang, Y., Cui, Y.L., Zhang, X.L., Yu, Q.B., Wang, X., Yuan, X.B., Qin, X.M., He, X.F., Huang, C., and Yang, Z.N. (2018). A nuclear-encoded protein, mTERF6, mediates transcription termination of rpoA polycistron for plastid-encoded RNA polymerase-dependent chloroplast gene expression and chloroplast development. Sci Rep 8, 11929.
Pubmed: Author and Title
Google Scholar: Author Only Title Only Author and Title

Zhao, Q., and Liu, C. (2017). Chloroplast Chaperonin: An Intricate Protein Folding Machine for Photosynthesis. Front Mol Biosci 4, 98.
Pubmed: Author and Title
Google Scholar: Author Only Title Only Author and Title

Zhao, Y., Cai, M., Zhang, X., Li, Y., Zhang, J., Zhao, H., Kong, F., Zheng, Y., and Qiu, F. (2014). Genome-wide identification, evolution and expression analysis of mTERF gene family in maize. PLoS One 9, e94126.
Pubmed: Author and Title
Google Scholar: Author Only Title Only Author and Title

Zhou, B., Zhang, L., Ullah, A., Jin, X., Yang, X., and Zhang, X. (2016). Identification of Multiple Stress Responsive Genes by Sequencing a Normalized cDNA Library from Sea-Land Cotton (Gossypium barbadense L.). PLoS One 11, e0152927.
Pubmed: Author and Title
Google Scholar: Author Only Title Only Author and Title

Zou, M., Mu, Y., Chai, X., Ouyang, M., Yu, L.J., Zhang, L., Meurer, J., and Chi, W. (2020). The critical function of the plastid rRNA methyltransferase, CMAL, in ribosome biogenesis and plant development. Nucleic Acids Res 48, 3195-3210.

Pubmed: Author and Title
Google Scholar: Author Only Title Only Author and Title